Title:

Altering Starch Digestion using crop genetics to improve glucose homeostasis in humans

Authors: Katerina Petropoulou[1‡††], Louise J. Salt[2‡††], Cathrina H. Edwards[2††], Frederick J. Warren[2††], Isabel Garcia-Perez[3], Natalia Perez-Moral[2], Kathryn L. Cross[2], Lee Kellingray[2], Rachael Stanley[2], Todor Koev[2,4], Yaroslav Z. Khimyak[4], Arjan Narbad[2], Nicholas Penney[3], Jose Ivan Serrano-Contreras[3], Edward S. Chambers[1], Rasha Alshaalan[1], Mai Khatib[1], Maria N. Charalambides[5], Jesus Miguens Blanco[6], Rocio Castro Seoane[6], Julie A. K. McDonald[6,7], Julian R. Marchesi[6,7,8], Elaine Holmes[3], Ian F. Godsland[9], Douglas J. Morrison[10††], Tom Preston[10††], Claire Domoney[11††], Peter J. Wilde[2††], Gary S. Frost[1*††]

Affiliations:

[1]Section for Nutrition Research, Department of Medicine, Imperial College London, London, W12 0NN, UK.

[2]Quadram Institute Bioscience, Norwich Research Park, Norwich, Norfolk, NR4 7UQ, UK.

[3]Computational and Systems Medicine, Division of Integrated Systems Medicine and Digestive Diseases, Department of Surgery and Cancer, Faculty of Medicine, Imperial College London, SW7 2AZ, UK.

[4]School of Pharmacy, University of East Anglia, Norwich Research Park, Norwich, NR4 7TJ, UK.

[5]Department of Mechanical Engineering, Imperial College London, London SW7 2AZ, UK.

[6]Division of Integrative Systems Medicine and Digestive Disease, Department of Surgery and Cancer, Imperial College London, W2 1NY, UK.

[7]Centre for Clinical Microbiome Research, Imperial College London, W2 1NY, UK.

[8]School of Biosciences, Cardiff University, Cardiff, CF10 3AX.

[9]Diabetes, Endocrinology and Metabolism, Department of Medicine, Imperial College London W2 1NY, UK.

[10]Scottish Universities Environmental Research Centre, University of Glasgow, East Kilbride, G75 0QF, UK.

[11]John Innes Centre, Norwich Research Park, Norwich, NR4 7UH, UK.

†† These authors contributed equally

‡ These authors have shared authorship

* To whom correspondence should be addressed:
Professor Gary Frost PhD RD
Nutrition Research Section
Division of Diabetes, Endocrinology and Metabolism
6th Floor Commonwealth Building
Faculty of Medicine
Imperial College Hammersmith Campus
Du Cane Road
London W12 ONN
Email g.frost@imperial.ac.uk

Abstract: Elevated postprandial glucose (PPG) is a significant driver of non-communicable diseases globally. Carbohydrate-rich foods are a major determinant of PPG. Currently there is a limited understanding of how starch structure within a food-matrix interacts with the gut luminal environment to control PPG. We use pea seeds (*Pisum sativum*), as a model-food, to explore the contribution of starch structure, food-matrix and intestinal environment on PPG. Using stable isotope [^{13}C] labelled seeds, coupled with synchronous gastric, duodenal and plasma sampling *in vivo*, we demonstrate that maintenance of cell structure and changes in starch morphology are closely related to lower glucose availability in the small intestine, resulting in acutely lower PPG and promoting changes in the gut bacterial composition associated with long term metabolic health improvements. This work offers huge potential to improve the design of food products targeted at moderating PPG and therefore lowering the risk of non-communicable diseases.

Introduction

The prevalence of non-communicable diseases such as obesity, type 2 diabetes (T2D), and coronary artery disease are rising, representing a major health and financial burden worldwide. Elevated post prandial blood glucose (PPG) is a major risk factor for T2D and associated metabolic diseases (O'Keefe and Bell, 2007). The consumption of carbohydrate rich foods is a major determinant of PPG response (Wolever and Bolognesi, 1996) and glycaemic index (GI) is a method used to rank carbohydrate rich foods according to their impact on PPG (Jenkins et al., 1981). Increasing intake of low GI foods that reduce PPG has been proposed as a successful strategy to improve metabolic health (Jenkins et al., 2002, Greenwood et al., 2013, Jenkins et al., 2008). However, the effect a carbohydrate-based food has on PPG is dependent on many factors such as: the physical structure of food, the type of carbohydrate (e.g., starch and dietary fibre) that it contains, the way the food has been processed and neural and hormonal cues in response to nutrient ingestion. Evidence indicates that the same food can result in different PPG and insulin responses depending purely on processing, for example, as in comparisons of native starch versus retrograded starch (Wang and Copeland, 2013).

Here, in a series of experimental studies, using normo-glycaemic volunteers to assess the potential primary prevention impact on metabolic disease, we explore the importance of food structure, carbohydrate quality, and the small intestinal environment on PPG and gut bacteria environment. Throughout, we used mature seeds of pea (*Pisum sativum L.*) as a model food. This crop species shows genetic variation and provides a great opportunity to investigate the impact of starch assembly on digestive processes. Specifically, we used two near isogenic pea lines, which were developed to be near identical genetically except that one line (BC1/19rr) carries a natural mutation in the starch branching enzyme I gene (*SBEI*) (Rayner et al., 2017). In BC1/19RR, the wild-type or control line, SBEI makes a major contribution to the amylopectin (branched starch) fraction present in pea seeds, where the enzyme is active within

the plastids of the cotyledonary cells (Fig. 1). The naturally occurring mutation in the *sbeI* gene (BC1/19rr) is caused by an insertion event which disrupts the carboxy-terminal region of the protein affecting the structure of the starch and other seed phenotypic traits (Bhattacharyya et al., 1990, Rayner et al., 2017). This genetic variant has been classified as the *sbeI-ins* allele and accounted for all *sbeI* mutants within a germplasm resource which was studied (Rayner et al., 2017). In the mutant line (BC1/19rr), the majority of the starch which is synthesised has been dubbed 'resistant starch', reflecting its largely unbranched amylose polymers and resistance to digestion. This naturally occurring mutation is unique in *rr* peas however mutations in SBE exist in other species, mainly induced, such as induce mutation in rice (Satoh et al., 2003) and in durum wheat (Hazard et al., 2012) given the observations made in this series of studies wide applicability targeting the production and use of commonly consumed foods high in 'resistant starch'.

In this work, we compared BC 1/19RR wild type and mutant BC 1/19rr peas to examine the effects of genetic alterations to starch structure on digestion parameters and associated health outcomes. Additionally, we explore the effects of processing and altered food structure by

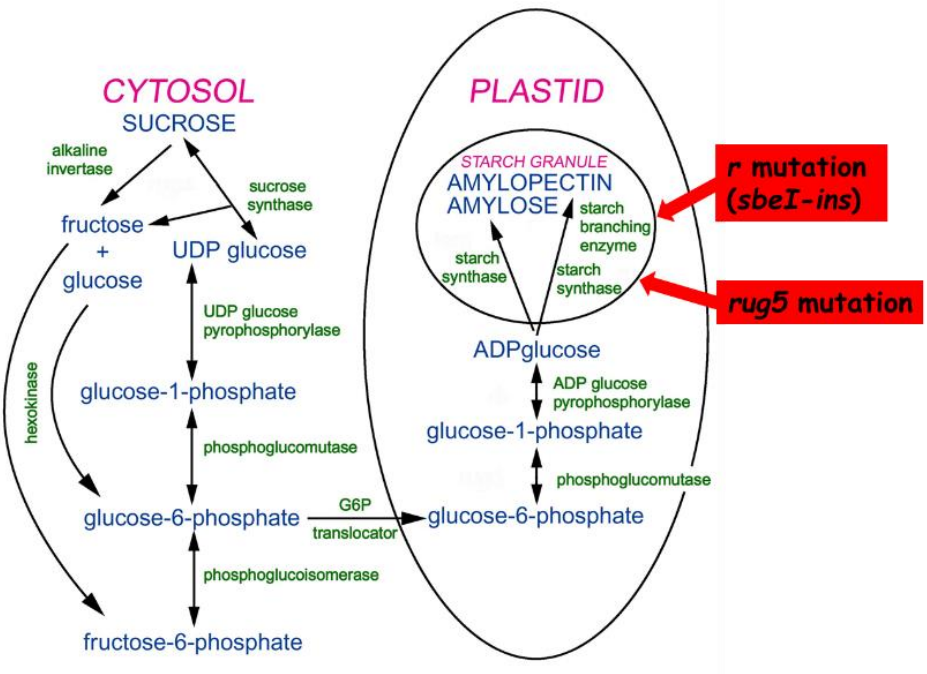

100 milling the pea seed to flour and by producing and pea-derived food products; this processing
101 resulted in disruption of the cell wall.

102 **Figure 1. Schematic of the starch biosynthetic pathway in pea seeds adapted from (Wang**
103 **et al., 1998).** The contribution of different enzymes to steps in the cytosol and within the plastid
104 and starch granule are shown in green with the metabolites in blue. The red boxes highlight
105 two mutations affecting enzymes which are active within the starch granule and influence
106 starch structure, of which the naturally-occurring *sbeI-ins* mutation is used in this study.

Results

rr starch genotype and food-structure reduce postprandial plasma glucose and serum insulin

We conducted an exploratory study in 10 healthy volunteers to assess the influence of cooked *RR* and *rr* whole pea seeds and flour on gastric emptying and to measure any possible differences, which might influence PPG response. In a mixed meal, we used 50 g dry weight of whole seeds or flour from two pea genotypes (BC1/19RR and BC1/19rr), providing 29% and 26% respectively of the total carbohydrate content of the meal. We assessed solid phase gastric emptying by the [^{13}C] octanoic acid breath test (Ghoos et al., 1993). There were no significant differences in baseline characteristics between groups (Table S1). Gastric emptying data for whole seeds and flour, as determined by $T_{½}$ (half-emptying time), are shown in Fig. 2A, B. There were no significant differences between the seeds (p=0.49) or flour groups (p=0.59) indicating that volunteers began digesting the two different test meals in a similar time course. However, there was a significantly lower PPG for both the seeds and flour meal compared to the *RR* (effect over time, p=0.02, p=0.04 respectively) Fig. 2C, D.

Next, to understand the impact of the pea genotype and structure on postprandial glycaemia and insulinaemia we undertook a study in 12 healthy volunteers. The effect of 50 g dry weight *RR* and *rr* seeds and derived flour, as cooked products alone, was tested. This experimental design was a pragmatic approach aimed at representing what a consumer might choose to eat in a real-life meal setting. Volunteer's characteristics are given in Table S2. For whole seeds, plasma glucose and serum insulin concentrations were significantly lower after consumption of *rr* compared to *RR* (effect over time, p=0.02 and 0.001 respectively) (Fig. 2E, F). There was no effect on glucagon-like peptide 1 (GLP-1) (Fig. 2G). The *RR* seeds consumption led to a

higher release of gastric inhibitory polypeptide (GIP) compared to *rr* (effect over time, p=0.01) (Fig. 2H).

With flour, we observed a lower PPG response after consumption of *rr* compared to *RR* that approached statistical significance (effect over time, p=0.06) (Fig. 2I). Serum insulin $iAUC_{0-120}$ was significantly reduced by 37% (p=0.04) for *rr* compared to *RR* (Fig. 2J). During the first 15 minutes' post ingestion, there was a higher peak in GLP-1 concentrations observed for *RR* compared to the *rr* group (p=0.001) (Fig. 2K). There was also a significantly higher $iAUC_{0-120}$ GIP for *RR* compared to *rr* (p=0.02) (Fig. 2L).

The increase in GLP-1 and GIP in both the *RR* peas and flour tests may be stimulated by the rapid increase in glucose, early in the digestive process. Changes in food structure, induced through processing whole seeds to flour within genotype, showed profound effects on PPG and serum insulin. In both *RR* and *rr*, processing to flour produced a significantly larger glucose and insulin response over 180 minutes (Fig. S1A-D). These observations support a major impact of plant cell structure on PPG and insulin. Together, these data demonstrate that both starch genotype and food structure have an impact on postprandial glycaemia.

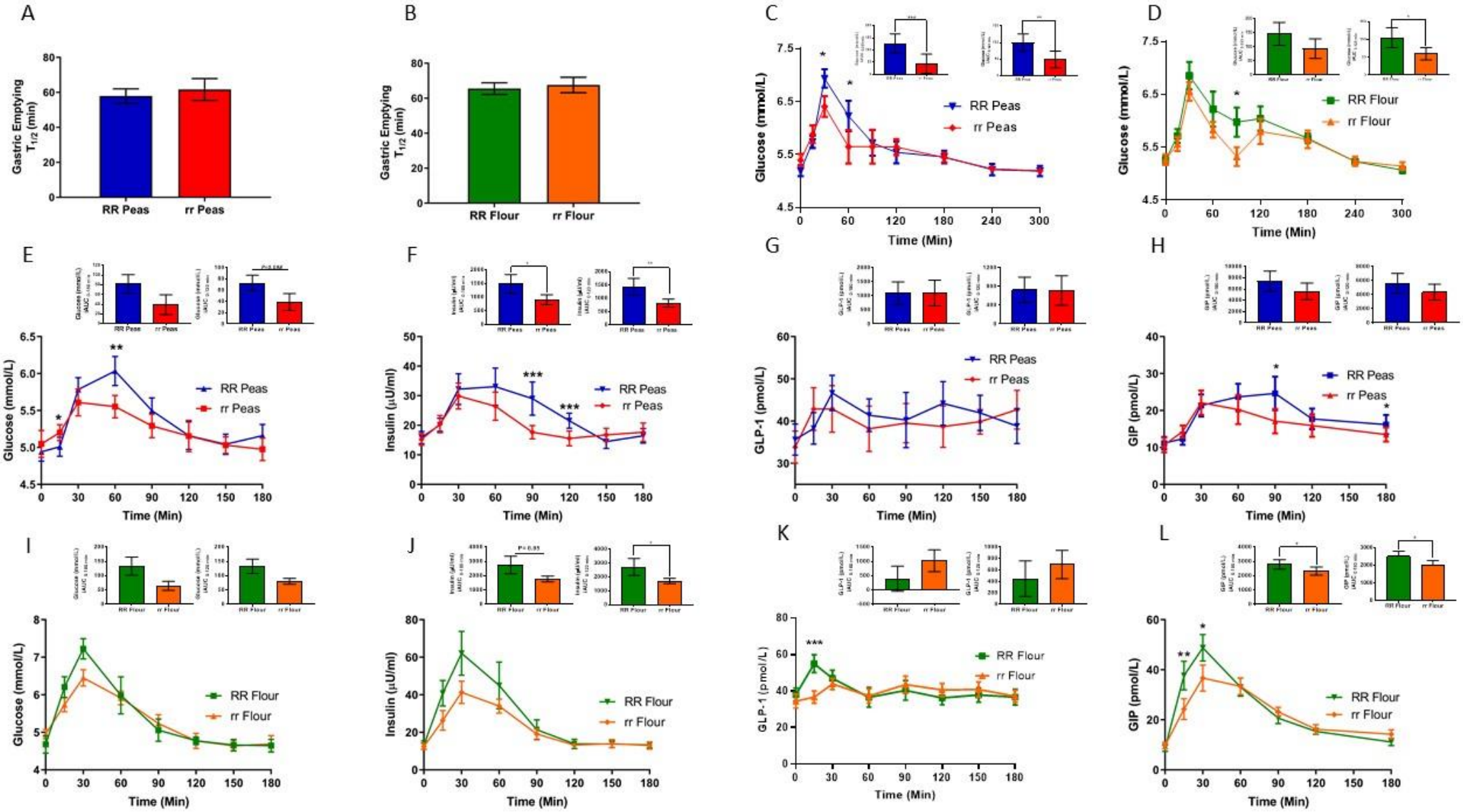
A
Gastric Emptying T1/2 (min)
RR Peas
rr Peas
B
Gastric Emptying T1/2 (min)
RR Flour
rr Flour
C
Glucose (mmol/L)
RR Peas
rr Peas
Time (Min)
D
Glucose (mmol/L)
RR Flour
rr Flour
Time (Min)
E
Glucose (mmol/L)
RR Peas
rr Peas
Time (Min)
F
Insulin (µU/ml)
RR Peas
rr Peas
Time (Min)
G
GLP-1 (pmol/L)
RR Peas
rr Peas
Time (Min)
H
GIP (pmol/L)
RR Peas
rr Peas
Time (Min)
I
Glucose (mmol/L)
RR Flour
rr Flour
Time (Min)
J
Insulin (µU/ml)
RR Flour
rr Flour
Time (Min)
K
GLP-1 (pmol/L)
RR Flour
rr Flour
Time (Min)
L
GIP (pmol/L)
RR Flour
rr Flour
Time (Min)

145

Figure 2. The effect of acute consumption of 50 g dry weight *RR* and *rr* pea seeds and flour.

t ½ was determined from the modelled [^{13}C] data in order to describe gastric emptying rates. $t_{1/2}$ was defined as the timepoint at which 50% of exhaled $^{13}CO_2$ is recovered. (A) Gastric emptying rates for *RR* and *rr* seeds consumption group (n=10). (B) Gastric emptying rates for *RR* and *rr* flour consumption group (n=10). (C, D,) Concentration of plasma glucose for *RR* and *rr* seeds and flour groups during a mixed meal experimental test. (E-H) Concentration of plasma glucose, serum insulin, GLP-1 and GIP measured for 180 minutes for *RR* and *rr* seeds group when fed alone (n=12). (I-L) Concentration of plasma glucose and corresponding serum insulin, plasma GLP-1 and GIP for *RR* and *rr* flour group. Analysis for flour was performed on available paired data, (n=11). Insets show the iAUC between 0 and 300/120 or 180/120 min. The data represent mean ±SEM. Repeated Measures Anova model was used for testing time course data with pea/flour and time as within-subject factors. Fisher LSD post-hoc tests were performed between timepoints when significant pea/flour$_x$time interaction was found. Paired *t*-tests were used for iAUCs calculations and gastric emptying data analysis. Timepoints at which values differed significantly, *p<0.05, **p<0.01, ***p<0.001. Abbreviations: iAUC, incremental area under the curve.

Impact of pea structure and starch assembly on starch digestion

To understand the impact of food structure and pea genotype on PPG and serum insulin observed *in vivo*, we undertook a series of experimental studies *in vitro* to decipher some of the physico-chemical mechanisms of starch digestion and nutrient bio-accessibility in *RR* and *rr* seeds.

Starch digestibility

The total starch contents of whole seeds and flour were determined for both genotypes, at raw state, post-cooking and post-simulated digestion (oral, gastric/small intestinal conditions) (Fig. 3A). As expected, the starch content of all samples decreased during simulated digestion. Less starch was digested in whole seeds, (60% for *RR* and 24% in *rr)* (Fig. 3A) indicating that that the starch in *rr* whole seeds was less digestible by the upper GI enzymes than the starch in *RR* whole seeds and corroborates the findings in Fig. 2 (significantly reduced glycaemic response when consuming *rr* peas).

After cooking, the portion of analytically resistant starch (ARS) content (Panwar et al.), based on the AOAC 2002.02 method, remained the same in both the *RR* and *rr* flour (Fig. 3B). Surprisingly, in whole seeds, the ARS content decreased in the *RR*, but increased in the *rr* after cooking and digestion. As this was an unexpected increse in ARS for *rr* whole seeds, ^{13}C cross polarized magic angle spinning (CP-MAS) NMR was used to establish the helical structure of the starch in uncooked and cooked pea seeds and flour, a key determinant of its resistance to digestion (Fig. 3C & Fig. S2) (Gidley et al., 1995, Lopez-Rubio et al., 2008).

The starch in the uncooked *RR* line presented a 35% double helical structure, in both the flour and whole seed (indicating that the starch was not significantly altered during milling), whereas the *rr* line had a lower proportion of double helices (19%), values similar to starch crystallinity

values determined previously for *RR* and *rr* pea lines, using x-ray diffraction (Fig 3C) (Bogracheva et al., 1995, Tahir et al., 2010).

Following cooking, the flours fully gelatinised, with starches from both genotypes (*RR* and *rr*) having less than 10% double helical order. In contrast to flour, starch from whole seeds of the *RR* genotype only partially gelatinised with a small decrease in double helical order (from 34% to 27%), whereas in the *rr* genotype there was an increase in double helical order observed following cooking (from 20% to 31%). This difference suggests a mechanism for the total starch and ARS analysis and an explanation for the marginal effects observed in PPG and serum insulin concentrations when the *RR* and *rr* flour was given to healthy volunteers, compared to *RR* and *rr* whole seeds.

We hypothesized that this process is analogous to annealing where, in the spatially and water limited environment of the plant cell, the starch undergoes structural rearrangements that are different to those in the flour, where the starch is unrestricted in terms of space and access to water. This spatial difference leads to significantly higher levels of ordered structures in the cooked whole seeds relative to cooked flours. These differences may be attributed to differences in the chain length distribution of the *rr* starch (Fig. 3D), which shows that the *rr* starch has far fewer short amylopectin chains (with an R_h of less than 4nm), and a greater proportion of longer amylose chains, which limits swelling of the starch and alters recrystallisation following cooling (Shrestha et al., 2010). The limited swelling and higher ordered structure following cooking (Fig. 3C and F) of *rr* starch as a result of greater long chain amylose leads to a greater proportion of starch escaping small intestinal digestion and reaching the colon where it would be available for fermentation by resident gut bacteria.

Impact of the food-matrix on processing and digestion

Simulated digestion experiments revealed that pea seed fragments (> 2 mm) formed from 'chewing' during the simulated oral phase remained intact and survived the digestion *in vitro*. Therefore, the size of the particles was measured post-gastric and intestinal phases. Fig. 3E shows that *rr* digesta contained a higher number of larger particles (> 700 μm) when compared to *RR*. A peak in the particle size distribution visible at around 100 μm (peak range 0-250 μm) shows that *RR* digesta contained a higher number of smaller particles than *rr* (such as individual cells, free starch and smaller fragments of pea tissue), suggesting that the cell matrix in *RR* was more friable than in *rr*. Interestingly, the size of the fragments did not change significantly during simulated digestion, as the results from the gastric and intestinal phases were similar, so the major impact on the structure was from cooking and the mechanical effect of simulated chewing.

The fracture profile of the cooked *RR* and *rr* seeds was investigated to better understand how the structure was affected by mechanical forces. Compression experiments using cooked whole seeds found that force-deformation curves were higher in *rr* compared to *RR* at 1mm/s ($p=<0.0001$) but were similar in both genotypes when the compression rate was increased to 15mm/s (Fig. 3H). The *rr* seeds fractured into larger particles of tissue in contrast to *RR*, where they appeared to breakdown completely (Fig. 3H). Although the moisture content for *rr* was higher than for *RR* seeds (60% vs 45%), it was noted that the physical appearance of compressed seeds was different; *rr* seeds tended to split while *RR* seeds were crushed (Fig. 3H). The greater resistance of the *rr* seeds to deformation can explained via the higher levels of insoluble fiber in the form of thicker or stronger cell walls (Skrabanja et al., 1999).

Micrographs of seed sections and flour demonstrated the impact of cooking (Fig. 3F, G) and simulated digestion (l Fig. S3) on the cellular structure and starch morphology. Micrographs of flour (iodine staining) demonstrated the influence of cooking on pea starch following the loss of the pea matrix by milling into flour. The raw starch granules of *rr* were very different

in morphology to those of the *RR* genotype (Fig. 3F). The *rr* starch granules were a mixture of simple and compound granules which is an effect of the high amylose content (Zhou et al., 2004). Starch from *RR* flour appeared to be almost fully gelatinized after cooking (Fig. 3F) and was no longer visible after digestion *in vitro* (Fig. S3). Together with the shorter chain lengths in RR (Fig. 3D), this probably explains the loss of total starch in RR flour following cooking, as the shorter chains probably leached out of the granules and may have avoided detection by the starch assay. However, intact starch granules from *rr* flour persisted throughout cooking, showing many intact, non-gelatinised granules (Fig. 3F) and following digestion *in vitro* (Fig. S3). After simulated duodenal digestion, however, the remaining *rr* flour granules were stained pink rather than blue.

Pea seed sections were stained with toluidine blue for protein and iodine for starch identification. After cooking, *RR* starch granules gelatinized to a greater extent than those of *rr* (Fig. 3G cooked), where the starch granules appeared less swollen. In the *RR* peas, starch appeared to be hydrolysed in some cells (where starch is lighter blue/ stained less) and not in others, after digestion *in vitro* (Fig. S3). On the other hand, starch granules in *rr* pea cells, that were less swollen after cooking, appeared undigested within the cells (Fig. S3). Scanning electron micrographs (Fig. S4) of uncooked and cooked seeds confirmed the extent of starch gelatinization within cotyledon cells seen with light microscopy. We observed starch granules to have gelatinized more extensively in *RR* peas and the starch appeared to have a furry texture, which could have formed when the starch expanded into the protein network surrounding it, and/or from amylose that had leached from the starch during cooking, an observation not seen in uncooked samples. In *rr* seeds, the protein network seems thicker and more extensive, the cell walls appear thicker and the interstitial regions have some different structural features, compared to *RR*. All these factors could impact on bio-accessibility and bio-availability during digestion *in vitro* and *in vivo* digestion.

Taken together the results show that there are at least two main factors which influence starch digestibility in the pea samples studied. Firstly, the structure and physico-chemical properties of the matrix, the latter of which are plant cell walls in seeds which encapsulate the starch and act as enzyme barriers while also hindering gelatinization of intracellular starch in whole peas, and secondly the intrinsic resistance of the starch granule. The higher amylose content of the *rr* genotype made it intrinsically more resistant to digestion due to its higher ARS content. Even though the rr starch in the flour lost much of its order, the morphology of the *rr* starch granules were affected to a lesser extent than *RR* starch following cooking. The matrix thus had an impact on several levels, in that there are marked differences between the *RR* and *rr* pea in carbohydrate profile, which is accentuated by cooking and digestion with differences in cell structure and fracture during digestion.

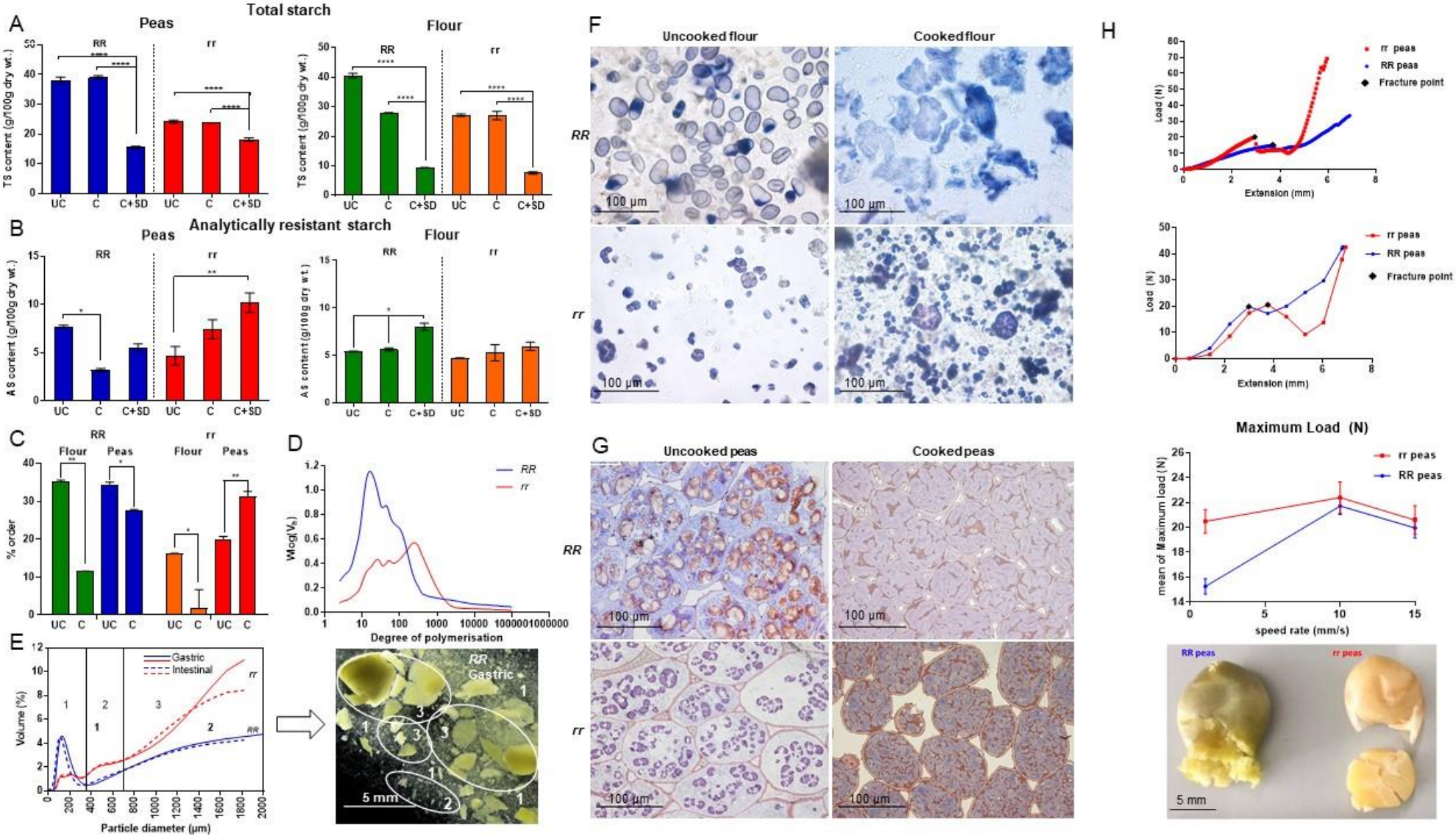
A
Total starch
Peas
Flour
RR
rr
TS content (g/100g dry wt.)
UC
C
C+SD
B
Analytically resistant starch
AS content (g/100g dry wt.)
C
% order
D
Mog(Vs)
Degree of polymerisation
RR
rr
E
Gastric
Intestinal
Volume (%)
Particle diameter (µm)
5 mm
F
Uncooked flour
Cooked flour
100 µm
G
Uncooked peas
Cooked peas
H
rr peas
RR peas
Fracture point
Load (N)
Extension (mm)
Maximum Load (N)
mean of Maximum load (N)
speed rate (mm/s)

264

Figure 3. The impact of genotype structure, and processing on starch digestibility.

(A, B) Total and analytically resistant starch (ARS) contents of uncooked (Zhang et al.), cooked (C) and cooked + simulated digested (C+SD) *RR* and *rr* whole seeds and flours. Structural characteristics of starch in uncooked and cooked flour and whole seeds; helical structure (C), chain length distribution (D). (E) Size of cooked whole seed fragments after simulated gastric and intestinal digestion. Micrographs of uncooked and cooked flours (F) and sections from uncooked and cooked whole seeds (G). Compression experiments (H) using hydrated/cooked *RR* and *rr* whole seeds. *p<0.05, **p<0.01, ***p<0.001. ****p<0.0001

rr genotype results in reduced small intestinal glucose release in humans

Since the results *in vitro* showed marked digestive differences between the *RR* and *rr* variants, we then explored the impact of the *rr* mutation on duodenal glucose release in humans. We intubated the small intestine and stomach of 12 healthy volunteers using nasogastric and nasoduodenal tubes. Firstly, we measured the glucose concentration in the small intestine after consumption of pea products (cooked whole pea seeds or flour). Small intestinal glucose concentration for the *RR* group, at 30 minutes, was 3.77 ± 2.28 mmol/L which was nearly two-fold higher than the *rr* group at the same time point (1.92 ± 2.21 mmol/L). We found that, in the *rr* group, small intestinal glucose release was lower and more attenuated during the time course of the study. Results from $AUC_{0\text{-}120}$ minutes indicated significantly higher small intestinal glucose concentrations for the *RR* compared with *rr* group (p=0.02) (Fig. 4B). We found no statistically significant differences in the small intestinal glucose responses between flours from the two pea genotypes (Fig. 4D).

Gastric and Small Intestinal Metabolic Profiles for Whole Pea Seeds

Next, we assessed the gastric and small intestinal metabolic profiles of the aspirated samples using Proton Nuclear Magnetic Resonance (^{1}H-NMR) spectroscopy. Statistically significant differences were found in the metabolic profiles of gastric samples when comparing *RR* and *rr* pea groups (Fig. 4E). Signals corresponding to the group of metabolites (full list Table S3, S4), amylopectin/maltotriose/maltose, were significantly higher for the *RR* samples at 30 minutes post ingestion compared with those of *rr* (p=0.0004, Q=0.002).

Metabolic profiles of small intestinal samples indicated differences between the two pea groups. We found statistically significant differences in glucose release rates, at 60 minutes post ingestion between the two pea groups (Fig 4F). *RR* seeds resulted in higher glucose release compared with *rr* (p=0.001, Q=0.01) (Table S5). The data suggests that leaching of

amylopectin/maltotriose/maltose from the *RR* seeds makes them more susceptible to early digestion and release of glucose.

Gastric and Small Intestinal Metabolic Profiles for Pea Flour

^{1}H-NMR metabolomic analysis of gastric flour samples indicated differences between the two pea genotypes (Fig. 4G). Similarly, to whole seeds, we found higher amylopectin/maltotriose/maltose in the gastric content of the *RR* flour group at 15- and 30-minutes post ingestion ($p=0.00004$, $Q=0.0019$/$p=0.0001$, $Q=0.0006$ respectively; Table S6).

In the small intestinal samples, the *RR* flour group showed higher glucose concentrations at 30 minutes compared to *rr* ($p<0.001$, $q<0.001$) (Fig. 4H). We also observed higher release of sucrose and alanine for *rr* flour compared to *RR* (Table S7).

α-amylase permeability in vitro and ex vivo

We used confocal microscopy to investigate the ingress of amylase into cooked peas and flour. Time course data showed that, within 10 min, FITC-amylase had diffused into the cell walls of both *rr* and *RR* peas (Fig. 4I) but not yet passed into the intracellular space. Further ingress of the enzymes into the intracellular space was slow, as captured by the diffusion constant (given by fluorescence intensity.nm^{2}.min^{-1}; 6.19 x 10^{-10} for *rr* and 1.23 x 10^{-9} *RR* (summarised in histogram, Fig. S5), and there was heterogeneity in plant cells obtained from *RR*, as seen in the time course (Fig. 4I). For flour, on the other hand, the amylase had bound to the surface of starch granules within 5 min and seemed to progressively erode the starch granules over time (Fig. 4.J). These experiments indicate that the encapsulation of starch by the cell wall obstructs interaction with amylase enzyme. The diffusion of amylase across the intracellular space appeared to be slower for *rr* than *RR* overall.

317 Using the small intestinal digesta from the study *in vivo* we performed experiments *ex vivo*
318 aiming to understand the cell wall permeability to α-amylase (AA) by following the diffusion
319 of AA labelled with FITC (FITC-amylase). In both *RR* and *rr* peas the diffusion of AA-FITC
320 into cells was progressive with time and that the diffusion of AA in *rr* pea samples was slower
321 than in *RR (*Fig. 4K). Uptake of AA-FITC into *RR* and *rr* pea flour was very quick, almost
322 immediate (Fig. 4K).

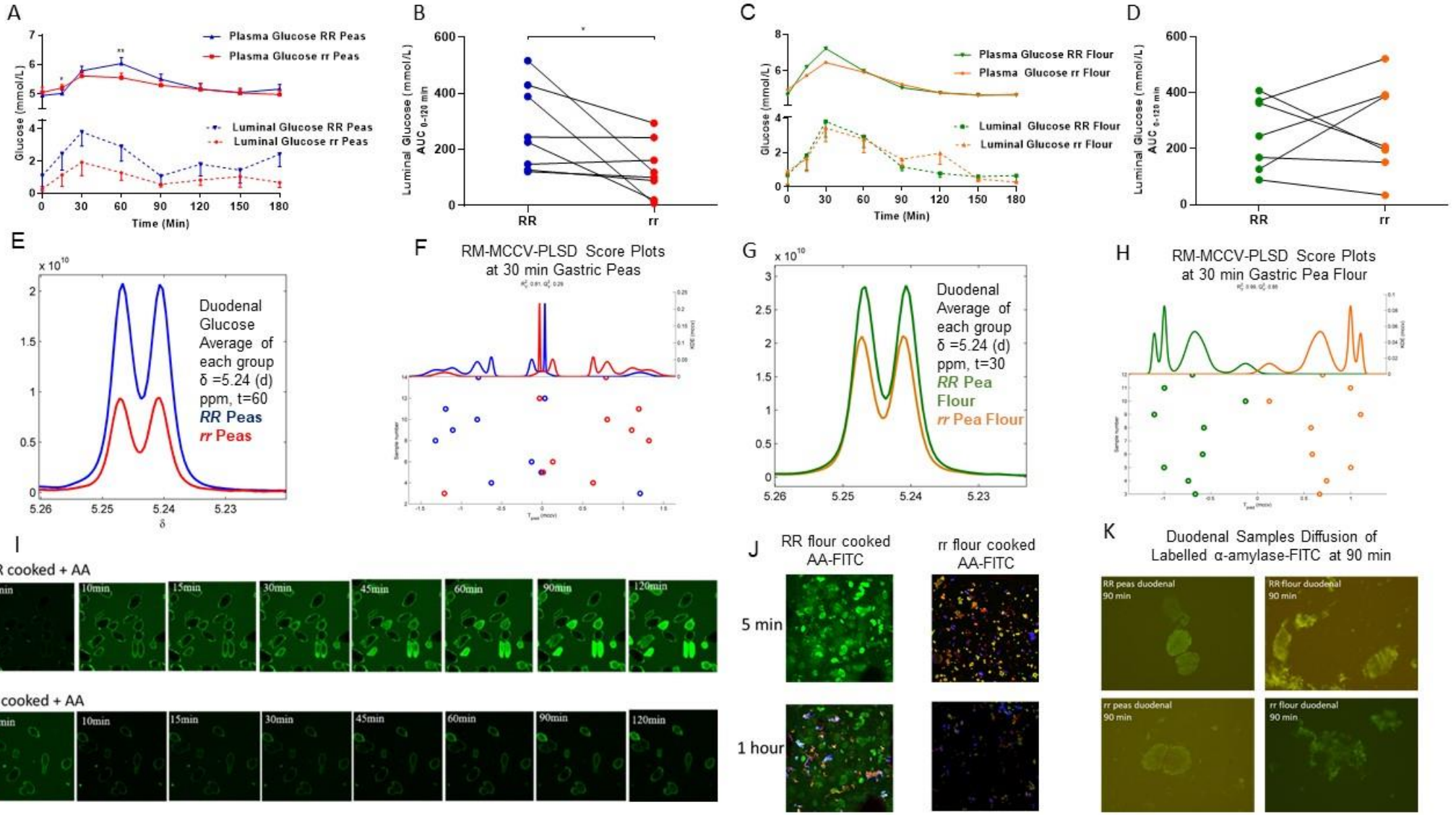
A
Plasma Glucose RR Peas
Plasma Glucose rr Peas
Luminal Glucose RR Peas
Luminal Glucose rr Peas
Glucose (mmol/L)
Time (Min)
B
Luminal Glucose (mmol/L) AUC 0-120 min
RR
rr
C
Plasma Glucose RR Flour
Plasma Glucose rr Flour
Luminal Glucose RR Flour
Luminal Glucose rr Flour
Glucose (mmol/L)
Time (Min)
D
Luminal Glucose (mmol/L) AUC 0-120 min
RR
rr
E
Duodenal Glucose Average of each group δ =5.24 (d) ppm, t=60
RR Peas
rr Peas
δ
F
RM-MCCV-PLSD Score Plots at 30 min Gastric Peas
G
Duodenal Average of each group δ =5.24 (d) ppm, t=30
RR Pea Flour
rr Pea Flour
H
RM-MCCV-PLSD Score Plots at 30 min Gastric Pea Flour
I
RR cooked + AA
rr cooked + AA
5min
10min
15min
30min
45min
60min
90min
120min
J
RR flour cooked AA-FITC
rr flour cooked AA-FITC
5 min
1 hour
K
Duodenal Samples Diffusion of Labelled α-amylase-FITC at 90 min
RR peas duodenal 90 min
RR flour duodenal 90 min
rr peas duodenal 90 min
rr flour duodenal 90 min

Figure 4. Small Intestinal Impact on structure and genotype of pea seeds and flour. (A) Postprandial small intestinal glucose curves for *RR* and *rr* pea seeds along with corresponding plasma glucose, where analysis was performed on available paired data, (n=8). (B) Individual responses expressed as $AUC_{0\text{-}120}$ for small intestinal glucose for whole seeds (n=8). (C) Postprandial small intestinal glucose curves for *RR* and *rr* flour along with corresponding plasma glucose, analysis was performed on available paired data, (n=7). (D) $AUC_{0\text{-}120}$ for small intestinal glucose for flour group (n=7). (E) RM-MCCV-PLS-DA scores plots of 1D ^{1}H-NMR gastric samples participants at 30 min after consumption of *RR* vs *rr* seeds (n=10). Model score: R^2Y 0.81, Q^2Y 0.29. Dots represent the metabolic profile of each volunteer from the study cohort; blue indicates *RR* and red indicates *rr* seeds. (F) Fragment from the average 600 MHz 1D ^{1}H-NMR spectrum of the *RR* (blue) vs *rr* (red) whole seeds showing the anomeric carbon signal (5.24 (d)) of the glucose molecule. (G) RM-MCCV-PLS-DA scores plots of 1D ^{1}H-NMR gastric samples comparing participants at 30 min after consumption of *RR* vs *rr* flour. Model score: R^2Y 0.99, Q^2Y 0.85. Dots represent the metabolic profile of each volunteer from the study cohort; green corresponds to *RR* and orange corresponds to *rr* flour. (H) Fragment from the average 600 MHz 1D ^{1}H-NMR spectrum of the *RR* flour (green) vs *rr* flour (orange) showing the anomeric carbon signal (5.24 (d)) of the glucose molecule. (I) Diffusion of labelled α-amylase-FITC in cooked *RR* and *rr* peas (green) at different timepoints. (J) Diffusion of labelled α-amylase-FITC in cooked *RR* and *rr* flour (green) at 5 and 120 min. (K) Diffusion of labelled α-amylase-FITC at 90 min in duodenal samples in *RR* and *rr* peas and flour.

Data are presented as mean ±SEM. Timepoints at which values differ significantly, *$p<0.05$, **$p<0.01$.

Abbreviations: AUC (area under the curve), RM-MCCV-PLSD (Repeated measures-Monte Carlo cross validation-Partial-squares-discriminant analysis), AA (α-amylase), FITC (Fluorescein isothiocyanate)

339 ***rr genotype increases SCFA production***

340 To understand the digestive process further, we labelled both the *RR* and *rr* seeds, with the
341 stable-isotope ^{13}C, by growing them in a $^{13}CO_2$ enriched environment in a hermetically sealed
342 greenhouse and assessed labelled metabolites in plasma and urine. This procedure produced
343 pea starch with an enrichment of ~0.2 atom percent ^{13}C above natural abundance. Volunteers
344 (n=10) undertook a randomised cross-over study to investigate ^{13}C glucose and ^{13}C SCFA
345 appearance after *RR* and *rr* seeds and flour consumption (Table S8, volunteer characteristics).
346 The time course and total area under the curve for exogenous ^{13}C postprandial plasma glucose
347 indicated significantly higher concentrations after consumption of the *RR* as opposed to the *rr*
348 seeds test meal (Fig. 5A, B). There was no significant effect observed when comparing *RR* and
349 *rr* flour for exogenous postprandial ^{13}C plasma glucose and total $AUC_{0\text{-}480}$ (Fig. 5C, D). These
350 observations support the PPG results observed in the first study (Fig. 2).
351 We measured fractional recovery of ^{13}C SCFA (acetate, propionate and butyrate) in 24-hour
352 urinary collections. ^{13}C acetate excretion did not result in statistically significant differences
353 between *RR* and *rr* in either the seed or flour groups (p=0.65). However, ^{13}C propionate and
354 ^{13}C butyrate output was significantly higher after consumption of *rr*, either seeds or flour
355 (p=0.01, p=0.03, respectively) (Fig 5E). This suggests that, with *rr* test meals, carbohydrate
356 was not fully digested in the small intestine and more was delivered to the colon where it was
357 fermented by the gut microbiota. We investigated whether or not changes in the stool gut
358 microbiome might occur over 24 hours but there was no difference in gut microbiome diversity
359 between the pea genotypes for either test meal (Fig. 5F).
360 These data suggest that the main effect on glucose absorption is the structural barrier of the
361 whole pea which is enhanced by the *rr* genotype. However, the SCFA production highlights
362 that the starch from the *rr* flour was not full digested in the small intestine. There was no

363 evidence of an acute effect on stool microbiota diversity although we observed an increase in

364 SCFA production with the *rr* genotype in both seeds and flour.

365

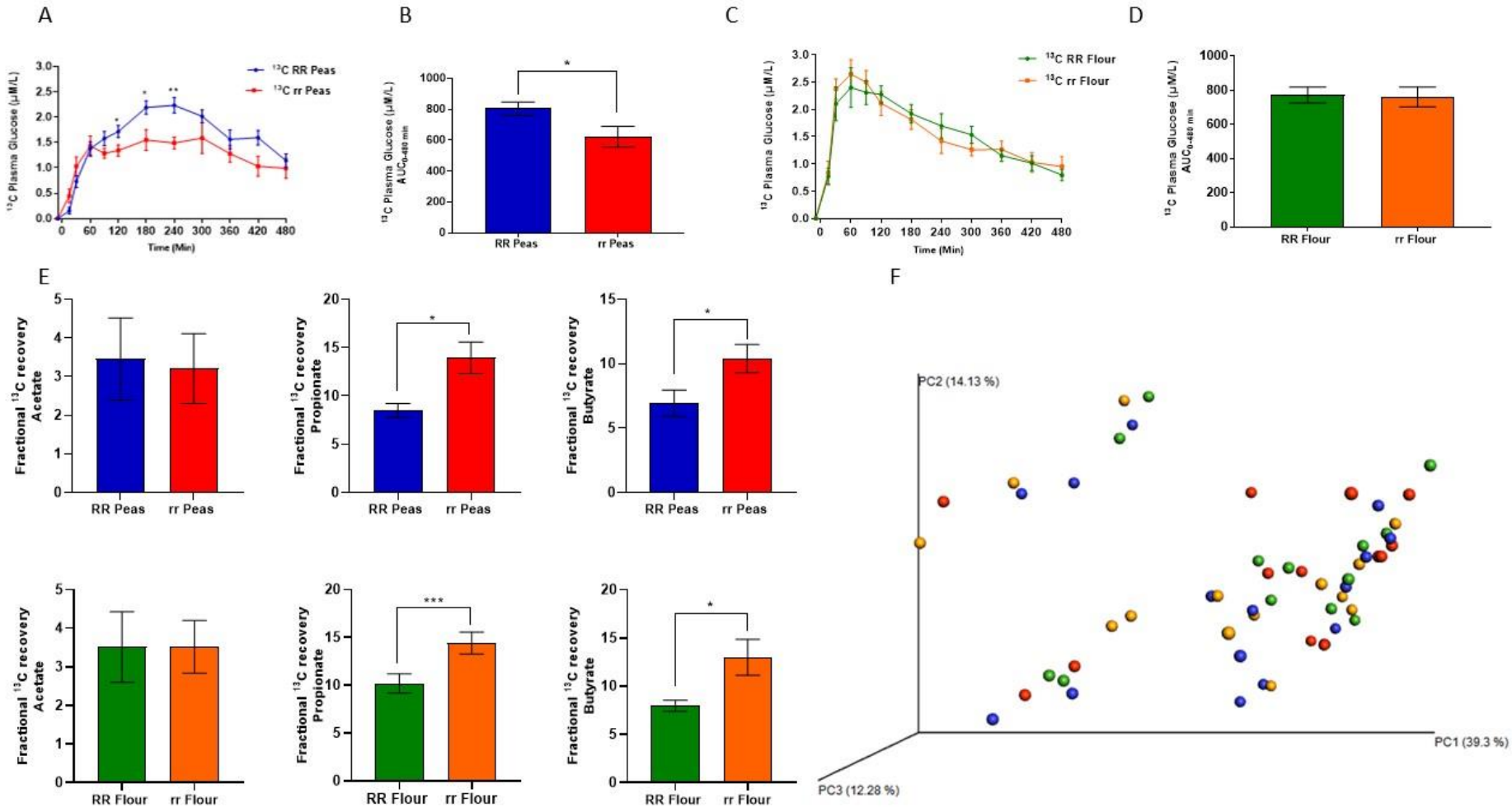
A
B
C
D
E
F
^{13}C RR Peas
^{13}C rr Peas
^{13}C RR Flour
^{13}C rr Flour
^{13}C Plasma Glucose (µM/L)
Time (Min)
^{13}C Plasma Glucose (µM/L) AUC$_{0-480\ min}$
RR Peas
rr Peas
RR Flour
rr Flour
Fractional ^{13}C recovery Acetate
Fractional ^{13}C recovery Propionate
Fractional ^{13}C recovery Butyrate
PC2 (14.13 %)
PC1 (39.3 %)
PC3 (12.28 %)

366

Figure 5. Using stable-isotope *^{13}*C-enriched *RR* and *rr* pea seeds and flour to understand the digestion and fermentation process further. (A) ^{13}C plasma glucose curves for *RR* and *rr* groups after administration of 50 g dry weight *^{13}*C-enriched whole seeds along with a mixed meal test (n=9). (B) Total $AUC_{0\text{-}480}$ of exogenous ^{13}C plasma glucose concentrations for *RR* and *rr* seeds (n=9). (C) Postprandial plasma ^{13} C glucose responses for *RR* and *rr* flour and (D) corresponding AUC (n=8). (E) Fractional enrichment in urinary concentrations of ^{13}C acetate, ^{13}C propionate and ^{13}C butyrate after consumption of ^{13}C-enriched *RR* and *rr* seeds (n=10) and flour (n=9). (F) Gut microbiota weighted beta-diversity plots for *RR* (blue) and *rr* (red) peas and *RR* (green) and *rr* (orange) flour. ^{13}C plasma glucose and urine samples were analysed using gas chromatography-combustion isotope ratio mass spectrometry. Beta diversity analysis was performed using the UniFrac metric calculated with QIIME 1.9.0 and visualized as a 3D principal coordinates analysis plot using Emperor. Data represent mean ±SEM. Repeated Measures Anova model was used for testing time course data with pea/flour and time as within-subject factors. Fisher LSD post-hoc tests were performed between timepoints when significant $pea/flour_x time$ interaction was found. Paired t-tests were used for AUC calculations. Time points at which values differ significantly, *$p<0.05$, *** $p<0.001$. Abbreviations: AUC, total area under the curve

Effect of *RR* versus *rr* pea seed products consumption on glycaemic control independently of the food matrix.

To understand the effects of the pea genotype independently of the food matrix on the PPG and gut bacteria we used a randomized, double-blind, crossover control trial in 25 metabolically healthy volunteers aged 40-70 years. Volunteer characteristics and a consort diagram are given in Table S9 and Fig. S6. Volunteers were provided with pea products to consume (mushy-peas/pea-hummus) for 28 days from the *RR* and *rr* lines in random order. They were asked to consume 1can of mushy peas (120 g) and 1 can of pea hummus (120 g) giving a daily increase of resistant starch of 20 g in the *rr* group. All measurements were performed at baseline (0 days) and follow up (28 days) after a 12 h overnight fast. We assessed the effects of repeated pea consumption exposure on stool gut bacteria, glucose metabolism, GLP-1 and lipids. A full summary of all outcome variables can be found in Table S10.

Glucose Metabolism

During the experimental procedure volunteers were given a mixed meal tolerance test without including the interventional pea-derived food product (both groups received the same meal). We found no statistically significant differences in markers of plasma glucose and serum insulin (fasting and postprandial measures) within or between groups (Fig 6A-D). Changes in β-cell function and insulin sensitivity were assessed by using the Homeostatic Model Assessment 2 (HOMA 2). We observed no differences within or between groups.

.

Gut Microbiome 16S rRNA Gene Sequencing

No statistically significant effect in the clustering within or between *RR* or *rr* interventions (within *RR*: p=0.83, within *rr*: p=0.92; between interventions: p=0.92) was observed (Fig. 6E). Due to high inter-individual variability we examined the data as paired samples per volunteer and looked specifically for gut bacteria related to insulin resistance. Within the *rr* intervention group, at genus level, there was a decrease in the relative proportion of *Bacteroides* (p=0.04) and an increase in the relative proportion of *Bifidobacterium* (p=0.007) between baseline and follow up (Fig 6F). Within the *RR* intervention group, results indicated a statistically significant decrease in *Lachnospiraceae* and *Ruminococcaceae* (p=0.01, p=0.004 respectively), which are known as starch degraders. Between groups (*RR* and *rr* interventions), a statistically significant decrease in the relative abundance of *Collinsella* was observed after 28 days of *rr* supplementation (p=0.03). Previous studies have reported increased levels of *Collinsella* in individuals suffering from T2D (Lambeth et al., 2015)

These data suggest that exposure to *rr* pea-derived products leads to positive changes in the gut bacteria associated with glycaemic control. However, there was no associated measurable impact of the genotype on blood glucose parameters in metabolically healthy volunteers over the relatively short 28 days supplementation period.

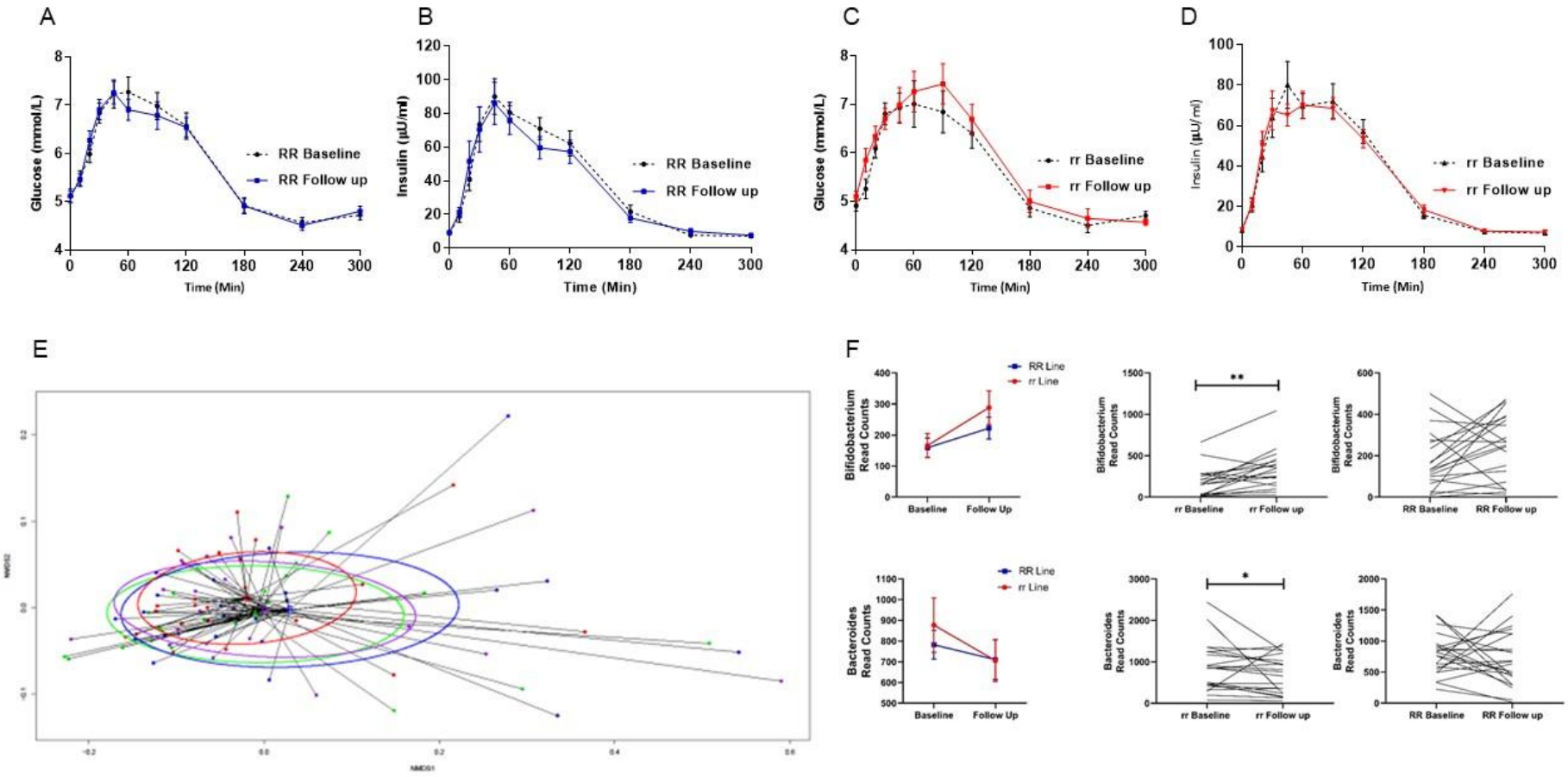
A
Glucose (mmol/L)
Time (Min)
RR Baseline
RR Follow up
B
Insulin (μU/ml)
Time (Min)
RR Baseline
RR Follow up
C
Glucose (mmol/L)
Time (Min)
rr Baseline
rr Follow up
D
Insulin (μU/ml)
Time (Min)
rr Baseline
rr Follow up
E
F
Bifidobacterium Read Counts
RR Line
rr Line
Baseline
Follow Up
**
rr Baseline
rr Follow up
RR Baseline
RR Follow up
Bacteroides Read Counts
*

417

Figure 6. The effect of consuming products derived from the two pea genotypes for 28 days on glucose homeostasis and gut microbiota. (A) Postprandial plasma glucose for *RR* and *rr* lines (B) and serum insulin responses: *RR* (C), *rr* (D). (E) Nonmetric multidimensional scaling (NMDS) plots for *RR* and *rr* pea interventions before and after the consumption of pea derived food products. *RR* visit 1; , *RR* Visit 2 , *rr* Visit 1 , *rr* Visit 2 . Analysis was performed on available paired data (n=22). Subsample read counts for Bifidobacterium and Bacteroides for both lines of peas (F).

Discussion

Drawing on insights from basic plant science and genetics, in this paper we provide novel insight on the impact of starch quality and food-matrix on human health, via the mutation at the *r* locus which results in a defective starch branching enzyme in *rr* compared with *RR* wild-type pea. The impact of the mutation on SBE activity results in differences in starch granule formation and digestion properties, leading to higher resistant starch content in the *rr* pea. We demonstrated that whole seeds and flour from the *rr* genotype made a significant impact on glucose and insulin homeostasis compared to the *RR* wild type and the most marked effect was seen when the cellular structures remained intact during digestion. Despite the fact that the difference in PPG between the *RR* and *rr* flour is less marked, we were able to observe a greater increase in fermentation in the case of *rr* flour. These observations align with other studies where bio-accessibility has been reduced in wheat endosperm with a concomitant decrease in PPG (Edwards et al., 2015). Recent reports have suggested that the starch granule of the *rr* seed has an outer layer of amorphous starch which is rapidly digested and an inner core of crystalline starch (Edwards et al., 2018). Others have shown that the initial rate of amylase digestion is the same between the genotypes, but decreases in the *rr* genotype over time (Tahir et al., 2010). It is possible that the lack of clear effect on blood glucose, in the case of flour, is related to the time in the duodenal space, which in humans is less than two hours. A possible explanation for these observations is that the amorphous starch in both genotypes is digested at the same rate during the time they are resident in the duodenum, and the resistant starch inner core, which is higher in the *rr* seed, is unaffected and delivered into the colon. We have demonstrated using direct measurements of glucose in the duodenum in humans that the availability of carbohydrate in the small intestine directly relates to plasma glucose concentrations. The more resistant starch structures in the whole *rr* seeds led to lower duodenal and lower PPG with a greater transfer of carbohydrate to the large bowel.

448 It is of interest that the higher availability of glucose in the duodenum from *RR* seeds is
449 associated with an increased release of GIP that relates to higher plasma insulin levels. This
450 increase is also reflected in the *RR* flour with higher post prandial levels of GIP and GLP-1
451 related to an increase in post prandial insulin. Duodenal glucose infusions in humans have
452 shown similar findings with high concentrations and flow rates of glucose in the duodenum
453 increasing both GLP-1 and GIP concentrations in the plasma (Pilichiewicz et al., 2007).
454 Although we did not observe a significant difference in direct measures of duodenal post
455 prandial glucose in the flour group, the NMR analysis suggests a higher duodenal glucose at
456 30 minutes. We conclude that postprandial insulin concentrations are higher in the *RR* whole
457 seeds and flour and this is driven through a higher availability of glucose in the small intestine
458 and the stimulation of the incretins, GIP and GLP-1. The reduction in duodenal glucose and
459 PPG in the face of lower insulin release but an increase in colonic fermentation in the *rr*
460 genotype would appear to be solely due to an increase in starch reaching the colon.

461 A series of experiments *in vitro* and *in vivo* demonstrated the complex multifactorial nature of
462 the increased delivery of starch to the colon in the *rr* genotype. Firstly, the cooked *rr* seeds
463 appear more resistant to fracture and during simulated gastric and duodenal digestion the size
464 of the particle population remained larger reducing the surface area for amylase activity
465 (Edwards et al., 2015, Edwards et al., 2018). Secondly, the metabolomic profiling of the
466 aspirated gastric and duodenal samples indicated differences between the two genotypes in the
467 amylopectin/maltotriose/maltose concentrations during digestion. It is known that amylopectin
468 is more readily digested than amylose and that amylose is a poor substrate for pancreatic α-
469 amylase (Zhang et al., 2006). Therefore, by identifying higher concentrations of these
470 metabolites in the digesta from the *RR* genotype it would suggest that the greater fracturing of
471 the food matrix in the *RR* genotype leads to increase in digestible carbohydrate in the
472 duodenum. Thirdly, we demonstrated that the complex nature of starch digestion and the size

and morphology and physical chemistry of starch granules (helix ordering and chain length) are more accurate predictors of glycaemic response than simply amylose content of the seed. For example, we demonstrated that cooking *rr* whole seeds increased amylose double helix starch structure, creating resistant starch that is not seen in *RR*. This process has been demonstrated to increase resistance to amylase previously (Gidley et al., 1995). Our data also suggest that the penetration of α-amylase into *rr* cells is lower and slower than in *RR* not only in the samples digested *in vitro* but in duodenal samples from humans *in vivo*, similar to observations made in ileostomy participants using wheat flour and particles (Edwards et al., 2015). The studies *in vitro* clearly align with the stable isotope experimental studies *in vivo* which demonstrate a reduced absorption of carbohydrate in the small intestine with an increase in bacterial fermentation in the *rr* compared with the *RR* group, as judged by fractional recovery in 24-hour urinary ^{13}C SCFA propionate and butyrate profiles. SCFAs, particularly butyrate, are associated with numerous health benefits (Donohoe et al., 2011). There was no detectable change in the stool 16S profile in the *rr* compared to the *RR* group at 24hours despite the increase in SCFA production. This suggests an increase in microbial carbon flux from the enrich carbohydrate colonic environment of the *rr* peas without an acute proportional change in microbiota species compared to *RR* peas. This effect was observed in both seeds and flour from the *rr* line highlighting the importance of the mutation on the starch compositional profile regardless of the food matrix, processing and preparation. These observations highlight the multicomponent aspect leading to reduced duodenal glucose.

Observations from the 28-day supplementation study, involving normo-glycaemic individuals, demonstrated positive changes in the gut microbiota with an increase in the proportion of the genus Bifidobacterium follow supplementation of the *rr* genotype. Studies have shown that Bifidobacterium abundance increase with enriched carbohydrate environment and has been associated with improvements and maintenance of metabolic health (Panwar et al., 2013). The

relatively short supplementation period coupled with the healthy cohort of volunteer used may explain why the changes in gut bacteria did not translate into improvements on markers of glucose homeostasis measured. It could be of interested to perform these experiments over longer duration and with individuals with impaired glucose tolerance or type 2 diabetes.

Our data shows that the impact of the contrasting genotypes on PPG it is due to complex differences in starch structure and food matrix and their impact on cooking and digestion. These observations could be used to inform the production of modified food types, either through the selection of digestion resistant starch phenotypes or altered food matrices with an aim to chronically lower PPG, which could reduce the number of individuals developing metabolic diseases at a population level.

Recent work on SBE genetic mutation has recently induced in staple crops such as rice and wheat, giving these results potential wide applicability, giving this work direct translation. With modern genetic and genomic tools, the discovery or generation of SBE mutations across a number of seed and grain crops provides great potential for expansion of such food products to tackle a major disease.

Materials and Methods

Food Materials

The food materials used during the experimental procedures are listed below:

1. Wild type pea seeds (BC 1/19RR line), used as control group
2. Mutant pea seeds (BC 1/19rr line), used as the treatment group
3. Wild type pea flour (BC 1/19RR line), used as control group
4. Mutant pea flour (BC 1/19rr line), used as treatment group
5. Wild type pea hummus and mushy peas (BC1/19RR line), used as control group
6. Mutant type pea hummus and mushy peas (BC1/19rr Line), used a treatment group.

The near-isogenic lines of pea (BC1/19RR, BC1/19rr) are available from the John Innes Centre Germplasm Resources Unit as accessions (JI3316 = *RR*, round-seeded, JI3317 = *rr*, wrinkled-seeded; https://www.seedstor.ac.uk). Bulked seed stocks were generated by growing plants on wire in field plots over successive seasons (March – July). The resulting seed stocks were used for studies *in vivo* and *in vitro* and supplied to the University of Glasgow for ^{13}C labelling and Campden BRI to produce the pea derived products. Campden BRI developed as provided the two pea products the long-term study.

^{13}C labelling of pea seeds: seeds were sown in troughs in a glasshouse at the James Hutton Institute, Dundee. The plants developed well and were pulse labelled with $^{13}CO_2$ one week after flowering. The mature seed was collected and air dried. A sub-sample of each variety was milled to a fine flour and analysed for crude protein, C:N ratio, total ^{13}C and starch ^{13}C. The yield of the wild type was 1.24 kg at 0.242 atom % ^{13}C excess, as measured by EA-IRMS at SUERC. The yield of the rr mutant was 1.26 kg at 0.133 atom % ^{13}C excess

Human Clinical Trials

Volunteers

All volunteers were provided with informed written consent forms prior to their participation in the 4 human clinical trial studies. All studies were approved by the South East Coast – Surrey Research Ethics Committee (15/LO/0184) and carried out in accordance with the Declaration of Helsinki. Volunteers were recruited via a healthy volunteer's database and public advertisement. For the exploratory studies 1, 2 & 3 men and women aged 18-65 years old, with a body mass index (BMI) of 18.5-29.9 kg/m^2 were recruited. For the 28-days study (study 4),

men and women 40 to 70 years old were recruited with same BMI as in studies 1, 2 & 3. Exclusion criteria for all studies included the following: weight gain or loss >3 kg in the previous 2 months, any chronic illness or gastrointestinal disorder, history of drug or alcohol abuse in the previous 2 years, use of antibiotics or medications likely to interfere with metabolic variable measured, smoking. All study visits took place at the National institute for Health Research/Wellcome Trust Imperial Clinical Research Facility, Hammersmith Hospital, London, United Kingdom and were conducted between May 2015 and December 2017. Randomization for all studies was generated by sealed envelope (Sealed Envelope Ltd, London, UK). In all human clinical studies volunteers were asked to consume the same standardized meal the evening before each study visit and avoid caffeine, alcohol consumption and strenuous exercise for 24 h before the experimental procedure. They were advised not to start any other new diets or intensive exercise regimes during the study period. Weight, height and body fat measurements were collected by using bioimpedance analysis (BC-418 Analyzer; Tanita UK).

Study 1-Study Day Protocol

This study was a randomized, controlled, double blind, cross-over trial. 10 volunteers were recruited for the study and attended 4 study visits (≥7days apart) after an overnight fast. Volunteers received a standardized test meal (0 min) with 50 gr dry weight of *RR* or *rr* pea seeds/flour in a random order. The test meal included 1 slice of white bread, 280 g tomato soup, 10 g butter and 1 microwaved egg with 100 mg ^{13}C-octanoic acid (Sercon Ltd, Crewe, UK) being injected in the yolk (378 kcal; 39 g carbohydrate, 18.6 g fat12 g protein and 2.7 g fiber). 50 g dry weight of pea seeds were soaked the day before in 200 ml of water and they were boiled the next morning for 1 hour in 1.8L of water. The pea seeds were added to the tomato soup along with the egg which contained 100 mg [^{13}C] octanoic acid. 50 g of dry weight flour was added to the tomato soup and was microwaved for 2 minutes. The flour and pea soup were then mixed with the egg which contained 100 mg [^{13}C] octanoic acid. ^{13}C-octanoic acid breath test is a non-invasive, reproducible, stable isotope method for measuring solid phase gastric emptying. By measuring the level of $^{13}CO_2$ that appears in breath samples following oxidation of the absorbed tracer, we were able to calculate how quickly the stomach empties after eating. Breath samples were taken every 15 min until the end of the study day (300 minutes). The breath test poses no risk to the volunteers and involves blowing through a straw into an Exetainer (Labco Co., High Wycombe, UK) until vapour condensed at the bottom of the tube. Analysis of breath $^{13}CO_2$ enrichment was by continuous flow isotope ratio MS (AP2003, UK).

Study 2-Study day Protocol

Twelve healthy volunteers were recruited for this randomized, controlled, double blind, cross over study. Volunteers had to attend the Clinical Research Facility for 4 consecutive days (3 nights). Nasogastric and nasoduodenal feeding tubes were placed to allow aspiration of samples from the stomach and small intestine. The enteral feeding tubes were placed by a doctor using the CORPAK (MedSystems, Halyard UK) feeding tube model that tracks the position of the tube during placement without the need for x-rays. The tubes remained in place for the duration of the 4-day visit. An intravenous cannula was inserted into one arm for blood sampling of plasma, serum and gut hormones. Each morning, fasting blood samples and gastric content samples were taken at –10 and 0 minutes. In random order, volunteers received at 0 min, a portion of 50 g dry weight *RR or rr* pea seeds and/or flour. Post prandial blood samples were collected at 15, 30, 60, 90, 120, 180 minutes.

Pea seeds and flour preparation: 50 g of dry weight peas and flour were soaked in 200ml of water 24 hours before each study visit. The morning before each study visit peas were boiled for 1 hour in 1.8 L of water. Flour was boiled for 40 min in 800 ml of water.

Study day Protocol – Study 3

Ten healthy volunteers were recruited for this randomized, controlled, double blind, cross over study and attended the research facility 4 times (≥7days apart) after an overnight fast. Volunteers received a test meal (0 min) which contained 50 g dry weight ^{13}C pea seeds/flour in random order. The test meal included 1 slice of white bread, 280 g tomato soup, 10 g butter (300 kcal; 39 g carbohydrate, 13.6 g fat, 6 g protein and 2.7 g fibre). Throughout the study volunteers were collecting urine samples and were advised to keep collecting their urine samples until the following morning (24 hours). The following morning, they returned to the research unit with the urine sample and a stool sample.

Pea seeds and flour preparation: 50 g dry weight peas were soaked in 200 ml of water 24 hours before the study visits, as in previous studies, and were boiled for 30 minutes the following day in 1.8L of water. 50 g dry weight of flour was added to the soup and was microwaved for 2 minutes as in previous studies.

Study day Protocol – Study 4

Twenty-five volunteers were recruited for this randomized, controlled, double blind, cross over study and attended the research facility for 4 visits. Volunteers had to undergo two separate 28-day supplementation periods and they were provided with mushy peas and pea hummus products (*RR* or *rr* line). Before and at the end of each 28-day supplementation period they attended the research facility for a study visit. At time (0) volunteers received an ENSURE drink (Ensure Vanilla Nutrition Shake, Abbott; 330ml, 66.6g carbs, 20.5g protein and 16.2g fat) consisting of 500 kcal. Blood samples were collected throughout the time course of the study (5 hours). Urine samples were collected for the same time frame. Volunteers had to collect a stool sample the day before each study visit. There was a 28-day washout period between the two supplementation periods.

^{13}C Breath Sample Analysis

Breath samples analysis was performed by isotope ratio mass spectrometry (IRMS) (Preston and McMillan, 1988). Breath samples were collected by exhalation of expired breath into an Exetainer (Labco Ltd, Lampeter, Ceredigion, United Kingdom) using a straw. Participants were encouraged to continue to blow into the Exetainer until condensate was observed in the base of the tube indicating alveolar breath collection (Edwards et al., 2002). Collected breath samples were analysed by flushing a portion of breath with helium gas into the IRMS where water is removed, and CO_2 separated from other gas species using gas chromatography before introduction into the mass spectrometer (AP2003, GV Instruments, Manchester, UK). The isotope ratio ^{13}C:^{12}C was calculated from the ion abundance of m/z 44, 45 and 46 with reference to a laboratory reference CO_2 (itself calibrated against Vienne Pee Dee Belemnite (*VPDB*)) with correction of the small contribution of $^{12}C^{16}O^{17}O$ at m/z 45, the Craig correction. Breath $\Delta^{13}C$ enrichment (‰) over baseline was calculated for each timepoint and the envelope of breath ^{13}C excretion was analysed using a modified version of the curve-fitting techniques to compute gastric emptying $T_{1/2}$ times (Ghoos et al., 1993).

Biological Sample Collection and Processing

Ten millilitres of blood were collected at each timepoint for assay of plasma glucose (EDTA), serum insulin, and plasma gut hormones (3 ml in lithium heparin tube containing 60 ul aprotinin protease inhibitor; Nordic Pharma UK). All blood sample tubes were centrifuged at 2500 X g for 10 min at 4^0C. Samples were separated and frozen at -80^0C until the end of the study where analysis took place.

637 Biological Sample Analysis

638 Glucose analysis was performed using Randox Glucose (GLU/PAP) kit supplied by Randox
639 using 20 ul of plasma glucose. A human insulin radioimmunoassay kit (Millipore) was used
640 for analysis of insulin based on manufacturer's specification with 50 ul serum. GLP-1 was
641 measured with the use of previously established in-house specific and sensitive
642 radioimmunoassay. GIP was measured by using an ELIZA Human GIP (Millipore) based on
643 manufacturer's specification with the use of 20 ul serum sample.

644 Experiments Ex Vivo

645 FITC labelled α-amylase was added to a suspension containing pea cells. Images of the cells
646 were taken at different time points using an Olympus BX 60 Fluorescence Microscope (Figure
647 X, I and J) or a Zeiss LSM 880 Confocal Laser Scanning Microscope (Figure Y and Z).

648 Metabolomic Gastric and Duodenal Samples Analysis

649 *Samples Extraction*

650 Gastric and duodenal samples were centrifuged for 15 minutes at 3000 X g. Metabolites were
651 extracted from the gastric and duodenal samples using a modified folch extraction procedure.
652 Two millilitres of chloroform/methanol in a 2:1 ratio was added to 450 ul of each gastric and
653 duodenal sample. This mixture was vortexed and 1ml of purified water was added. Samples
654 were vortexed for 1 minute and centrifuged for another 20 min at 3000 X g, at 0° C. This
655 method produced two phases and metabolites split into the aqueous and the organic phase
656 according to their polarity. The aqueous phases were separated and evaporated to dryness using
657 a speed vacuum concentrator and the dried sample was stored at -80^{o}C prior analysis. The NMR
658 profiles of the stomach and duodenal digested samples were analyzed by ^{1}H high resolution
659 NMR spectroscopy.

660 *Sample treatment*

661 The dried aqueous phase of the gastric samples was re-constituted in 540 ul of H_2O and were
662 sonicated for 20 minutes. 540 ul were mixed with 60 ul of a 3M phosphate buffer (pH 7.4, 80%
663 D_2O) containing 1 mM of the internal standard, 3-(trimethylsilyl)- [2,2,3,3,$^{-2}H_4$]-propionic acid
664 (TSP) were added and the mixture was transfer to the 5mm NMR tubes. The dried aqueous
665 phase dried of the duodenal samples were re-constituted in 640 ul of H_2O and were sonicated
666 for 20 minutes. 540 ul were mixed with 60 ul of a 1.5M phosphate buffer (pH 7.4, 80% D_2O)

containing 1 mM of TSP were added and the mixture was transfer to the 5mm NMR tubes. Quality control samples were prepared independently for gastric and duodenal samples by pooling 90 ul of each sample.

^{1}H-NMR Metabolic profiling analysis

^{1}H-NMR spectroscopy was performed on the aqueous phase extracts at 300 K on a Bruker 600 MHz spectrometer (Bruker Biospin, Karlsruhe, Germany) using the following standard one-dimensional pulse sequence with saturation of the water resonance RD – gz,1 – 90° – t – 90° – tm – gz,2 – 90° – ACQ (noesygppr1d) where RD is the relaxation delay, where 90° represents the applied 90° radio frequency (rf) pulse, t1 is an interpulse delay set to a fixed interval of 4μs, RD was 2 s and tm (mixing time) was 100 ms. Water suppression was achieved through irradiation on the water signal during RD and tm. For the gastric and duodenal samples, each spectrum was acquired using 4 dummy scans followed by 32 scans and collected into 64K data points. A spectral width of 20,000 Hz was used for all the samples. Prior to Fourier transformation, the FIDs were multiplied by an exponential function corresponding to a line broadening of 0.3 Hz. ^{1}H NMR spectra were manually corrected for phase and baseline distortions and referenced to the TSP singlet at δ 0.0. Spectra were digitized using an in-house MATLAB (version R2014a, The Mathworks, Inc.; Natwick, MA) script. Spectra were subsequently referenced to the internal chemical shift reference (trimethylsilyl- [2,2,3,3, $^{-2}H_4$]-propionate, TSP) at δ 0.0. Spectral regions corresponding to the internal standard (δ -0.5 to 0.5) and water (δ 4.57 to 5.18) were excluded. All spectra were normalised using median fold change normalisation using the median spectrum as the reference and imported into MatLab to conduct multivariable statistical analysis. Data were centred and scaled to account for the repeated measures design and then modelled using partial-least-squares– discriminant analysis (PLS-DA) with Monte Carlo cross-validation (MCCV). The fit and predictability of the models obtained were determined and expressed as R^2Y and Q^2Y values, respectively.

NMR Compound Identification

A combination of data-driven strategies such as Statistical TOtal Correlation SpectroscopY (STOCSY) and SubseT Optimization by Reference Matching – (STORM) and a catalogue of 1D ^{1}H NMR sequence with water pre-saturation and 2D NMR experiments such as *J*-Resolved spectroscopy (jresgpprqf), ^{1}H–^{1}H TOtal Correlation SpectroscopY (TOCSY (mlevphpr.2)), ^{1}H–^{1}H COrrelation SpectroscopY (COSY (cosygpprqf)), ^{1}H–^{13}C Hetero-

699 nuclear Single Quantum Coherence (HSQC (hsqcetgpsisp2.2)) and ^{1}H–^{13}C Hetero-nuclear
700 Multiple-Bond Correlation (HMBC (hmbcgplpndprqf)) spectroscopy were applied to identify
701 metabolites for the gastric and duodenal samples. Additional experiments were conducted in
702 order to acquire enhanced spectra by reducing the overlap mainly on the carbohydrate
703 resonances of the chemical shift region. The gradient-enhanced multiple-quantum-filtered
704 COSY pulse sequence (cosygpmfqf) was used to acquire both double-quantum-filtered and
705 triple-quantum-filtered COSY experiments in order to simplify cross peaks by filtering out
706 uncoupled protons and artifact peaks. ^{1}H-^{13}C multiplicity-edited HSQC (hsqcedetgpprsisp2.3)
707 spectrum was also acquired to differentiate methines (-CH-) and methyls ($-CH_3$) from
708 methylenes ($-CH_2-$). 2D-NMR experiments were acquired using their corresponding pulse
709 sequences with water presaturation during relaxation delay. Selective 1D TOCSY (selmlgp)
710 experiments were also obtained.

711 Objective assessment of peas intake

712 Urine samples were collected at baseline and follow up visits of the 28 days pea
713 supplementation period. Briefly, 540 ul of urine samples were mixed with 60 ul of a pH 7.4
714 phosphate buffer containing 1 mM of the internal standard TSP as previously described. ^{1}H-
715 NMR spectroscopy was performed on the urine samples at 300 K on a Bruker 600 MHz
716 spectrometer (Bruker Biospin, Karlsruhe, Germany) using the following standard one-
717 dimensional pulse sequence with saturation of the water resonance RD – gz,1 – 90° – t – 90° –
718 tm – gz,2 – 90° – ACQ (noesygppr1d) using an established method. ^{1}H NMR spectra were
719 manually corrected for phase and baseline distortions and referenced to the TSP singlet at δ
720 0.0, using an in-house MATLAB (version R2014a, The Mathworks, Inc.; Natwick, MA) script.
721 Urinary trigonelline was identified in the 1D ^{1}H-NMR spectra at δ 9.13(s), δ 8.84(t) and δ
722 4.44(s). Trigonelline quantification was performed as previously described (Garcia-Perez et
723 al., 2016).

724 Quantification of ^{13}C plasma glucose

725 Plasma samples were diluted 1:5 with L-fucose internal standard. The ^{13}C natural abundance
726 of L-fucose was separately calibrated against VPDB and used as a chemical and isotopic
727 internal standard. 0.5 ml of plasma was diluted with 2 ml internal standard. Samples then
728 underwent ultrafiltration using 30000 molecular weight cut-off ultrafiltration devices (Amicron
729 Ultra 4; Millipore, Watford, UK) at 3600 X g for 45 minutes to remove proteins and other high
730 molecular weight compounds. After this step, the samples were stored in two separate aliquots

731 at -20°C for further analysis. Analysis by liquid chromatography-IRMS (LC-IRMS) was
732 performed as previously described. Fucose and glucose peak areas and background-corrected
733 isotope ratios were exported to a spreadsheet for analysis. Glucose enrichment (δ ^{13}C (‰) was
734 calculated using an in-house routine using a relative ratio analysis approach against the IS for
735 each sample to report the enrichment of glucose relative to VPDB and glucose ^{13}C
736 concentration was calculated as the product of enrichment x concentration at each time point.
737 Glucose concentration was calculated from the area ratio of the glucose peak area relative to
738 fucose.

739 Quantification of ^{13}C SCFAs in urine samples

740 Samples were analysed using procedure from previously described (Morrison et al., 2004)
741 which was modified to increase sensitivity of the analysis. In brief, urine samples (7 ml) were
742 spiked with 200 nmoles 3-methyl valerate (3mV; internal standard) and 200 □L NaOH (300
743 mmoles/L). A 'process blank' was prepared containing freshly deionized water and identical
744 spikes of 3mV and NaOH. Samples and blanks for each run were dried on a vacuum
745 concentrator (Jouan RC10 Vacuum Centrifuge, ThermoFisher, Paisley, UK) at ambient
746 temperature. Dried samples were acidified with 100 □l HCl and SCFA extracted with 400 ul
747 methyl-tert butyl ether. 300 ul of the MTBE phase was removed to clean vials for analysis by
748 GC-C-IRMS as previously described (Morrison et al., 2004). The isotopic enrichment of each
749 SCFA was calculated relative to 3mV which itself had been calibrated against laboratory
750 standards and VPDB. Enrichment of each SCFA with time was expressed relative to the
751 enrichment of the starting pea material ingested to derive a fractional ^{13}C enrichment curve for
752 each SCFA.

753 Bacterial Composition Analysis of Stool Samples collected for study 3

754 Total DNA was extracted from stool samples (~200 mg) using the FastDNA SPIN Kit for Soil
755 (MP Biomedicals, UK) with a bead-beating step (Kellingray et al., 2017). DNA yield was
756 quantified using the Qubit fluorometer prior to the samples being sent to the Earlham Institute
757 (Lindström et al.), where the V4 hypervariable region of the 16S rRNA genes were amplified
758 using the 515F and 806R primers with built-in degeneracy (Caporaso et al., 2011). The
759 amplicons were sequenced using paired-end Illumina sequencing (2 × 250 bp) on the MiSeq
760 platform (Illumina, USA). Sequencing data were analysed using the Quantitative Insights Into
761 Microbial Ecology (QIIME) 1.9 software and RDP classifier 16S rRNA gene sequence
762 database (Wang et al., 2007). The trimmed reads were filtered for chimeric sequences using

ChimeraSlayer, bacterial taxonomy assignment with a confidence value threshold of 50% was performed with the RDP classifier (version 2.10), and trimmed reads clustered into operational taxonomic units at 97% identity level. Weighted and unweighted UniFrac distances were used to generate beta diversity principal coordinates analysis plots, which were visualised using the Emperor tool.

Bacterial Composition Analysis of Stool Samples collected for study 4

Stool samples were collected at baseline and follow up at each supplementation period. The samples were stored at -80^0C for between 6-9 months before processing. DNA was extracted from approximately 250 mg of stool samples using the PowerLyzer PowerSoil DNA Isolation Kit (Mo Bio, Carlsbad, CA, USA) following manufacturer's instructions. Samples were bead beaten for 3 min at speed 8 in a Bullet Blender Storm (Chembio Ltd, St. Albans, UK) and this was the only modification to the protocol. All samples were analysed in a single batch. Sample libraries were prepared by amplifying the V1-V2 region of the 16S rRNA gene following Illumina's 16S Metagenomic Sequencing Library Preparation Protocol with the following alterations. First, the index PCR reactions were cleaned up and normalised using the SequalPrep Normalization Plate Kit (Life Technologies, Paisley, UK). In addition, sample libraries were quantified using the NEBNext Library Quant Kit for Illumina (New England Biolabs, Hitchin, UK). Sequencing was performed on an Illumina MiSeq platform (Illumina Inc., Saffron Walden, UK) using the MiSeq Reagent Kit v3 (Illumina) using paired-end 300bp chemistry. The resulting sequencing data was processed following the DADA2 pipeline as previously described. The SILVA bacterial database version 132 was used to classify the sequence variants. The UniFrac weighted distance matrix generated from Mothur was used to generate non-metric multidimensional scaling (NMDS) plots and PERMANOVA p-values using the Vegan library within R (Dessau and Pipper, 2008). Due to high inter-individual variability we examined the data as paired samples per volunteer. Differences in microbial communities between and within groups were tested by using the Wilcoxon signed-rank test.

Digestion *In Vitro* - Study Design

Peas Preparation

Pea seeds were milled into a flour using an electric coffee grinder (Krups, Berkshire, UK), and were passed through a 1mm test sieve (Cole-Palmer, St. Neots, UK). All chemicals, reagents and enzymes were supplied by Sigma Aldrich (Dorset, UK) unless stated otherwise.

Approximately 5 g dried pea seeds were weighed and soaked overnight in 100 mL ultrapure water at room temperature. After soaking, the water content of the peas was approximately 60 % for the *rr* peas and 45 % for the *RR* peas. For the flour, 1 g flour was weighed into a Pyrex 15 mL glass tube (screw cap with PTFE cap liner) and mixed with an excess of ultrapure water (4:1). Samples were hydrated for 1 h at room temperature, then cooked for 1 h in a boiling water bath, cooled to room temperature and more water was added to the viscous mixture (8:1). The peas were boiled for 1 h in ultrapure water and drained, and the skins/testa were removed from both uncooked and cooked peas and then they were pushed through a garlic press (Lakeland, UK) with 2.5 mm dimeter holes. This step attempted to mimic chewing and produced chunks with particle sizes up to 2.5 mm.

Simulated digestion

Triplicate digestions of flours and pea chunks were carried out using a standardised static biochemical model developed by Minekus et al (2014) (Minekus et al., 2014). However, the compositions of the simulated digestion fluids were modified from the protocol described by Minekus et al (2014). In all cases sodium bicarbonate and ammonium bicarbonate were directly substituted with bis-tris, because bis-tris has a high buffering capacity which was particularly important for maintaining pH 7.0 (approximately) in the intestinal phase in sealed tubes, where regulation of pH by titration of 0.1M NaOH was not possible. The same simulated fluids were used for all experiments and all enzymes were purchased from Sigma-Aldrich Company Ltd., Dorset, UK).

Oral phase: simulated salivary fluid (SIF) [15.1 mM KCl, 3.7 mM KH_2PO_4, 13.66 mM bis-tris, 0.15 mM $MgCl_2(H_2O)_6$, 1.5 mM $CaCl_2(H_2O)_2$] was added, 1:1 v/w, to the samples immediately followed by human salivary amylase (product code A1031: type XIII-A lyophilised powder – α-amylase from human saliva) to give a final concentration of 75 U/ mL, and was incubated for 2 min at 37 °C.

Gastric phase: at 2 min, the sample was adjusted to pH 3.0 (± 0.05) using 0.1M HCl, simulated gastric fluid (SGF) [6.9 mmol KCl, 0.9 mmol KH_2PO_4, 25.5 mmol bis-tris, 47.2 mmol NaCl, 0.1 mmol $MgCl_2(H_2O)_6$, 0.15 mmol $CaCl_2(H_2O)_2$] was added (1:1 v/v). Finally, pepsin (product code P7012: pepsin from porcine gastric mucosa) was added to the digestion mixture to give a final concentration of 2000 U/ mL, and the gastric phase was incubated at 37 °C in a shaking incubator for 1 h. The recommended time for gastric digestion described by Minekus et al

(2014) is 2 h, however this time was reduced to 1 h, for these experiments, based on the lack of starch degrading enzymes in the gastric phase.

Intestinal phase: immediately after completion of the gastric phase the pH was raised to 7.0 (± 0.05) using 0.1M NaOH, simulated intestinal fluid (SIF) was added [6.8 mM KCl, 0.8 mM KH_2PO_4, 85 mM bis-tris, 38.4 mM NaCl, 0.33 mM $MgCl_2(H_2O)_6$, 0.6 mM $CaCl_2(H_2O)_2$, and 10 mM bile] (1:1 v/v) and finally pancreatin (product code P7545: pancreatin from porcine pancreas) was added to give a final concentration of 100 U/ mL. The intestinal phase was incubated at 37 °C in a shaking incubator (170 rpm) for 2 h.

Flour was digested in an open, heated mixing vessel where samples were stirred continuously (500 rpm) at 37 °C. The pH of the intestinal phase was maintained at 7.0 by KEM AT-700 automatic titrator (Kyoto Electronics, Leeds, UK). At the end of each phase of digestion, 0.1 mL samples were taken: oral phase 2 min; gastric phase 60 min, intestinal phase 120 min.
Pea chunks were digested in disposable centrifuge tubes (Greiner Bio-One Ltd, Stonehouse, UK). The chunks were too large to aspirate and so to overcome this, one centrifuge tube contained one sample for each time point. Pea chunks were digested at 37 °C in an orbital shaking incubator (Sartorius, Goettingen, Germany) at 170 rpm, and sample collection times were the same as for the flour.

Starch assay

Uncooked and cooked pea chunks (100 mg ±5 mg) were weighed into 15 mL centrifuge bottles and were digested according to the protocol described in section 3.2. The liquid phase was removed from the samples by centrifugation (2000 x g for 5 min) and careful aspiration by pipette. Additional digested samples were homogenised at 1000 rpm, using a T25 Ultra-Turrax (IKA, Oxford, England), post-intestinal digestion phase, to check that all starch in the pea chunks had been accounted for by the assay. The samples were milled (in digestion fluid) until no more chunks were visible, the ultra-turrax tip was washed with ultra-pure water and the washings were combined with the milled sample. The sample was centrifuged at 10000 x g for 10 minutes and the supernatant was aspirated, very carefully, by pipette.

Total and resistant starch contents of undigested and digested flours, pea biscuits and pea chunks were determined using assay kits purchased from Megazyme International (Co. Wicklow, Ireland).

Total starch (assay procedure K-TSTA 07/11). Samples were heated in aqueous ethanol (80% v/v) at 80-85 °C for 5 min, centrifuged at 1800 x g, 10 min. Supernatants were decanted, and excess liquid was drained from the pellets.

Resistant starch (assay procedure: KRSTAR 09/14). Samples were incubated with 4.0 mL pancreatic α-amylase (30 U/mL) and AMG (3 U/mL) for 16 h at 37 °C with continuous shaking (200 rpm), during which time non-resistant starch was solubilised and hydrolysed to D-glucose. Enzymes were halted by washing with 4.0 mL ethanol (99 % v/v), followed by centrifugation at 1500 X g for 10 min. Supernatants were decanted and pellets were re-suspended in 8.0 mL 50 % ethanol and the centrifugation step was repeated, and followed by a final washing step. Supernatants were decanted, and excess liquid was drained from the pellets.

All pellets were incubated in 2.0 mL 2 M KOH for 20 min on ice, neutralised in 8.0 mL 1.2 M sodium acetate buffer (pH 3.8). Starch was hydrolysed to form maltodextrins by addition of thermostable α-amylase to give a final content of 3.0 U/mL. The maltodextrins were further hydrolysed by addition of AMG to give a final content of 3.3 U/mL, to form D-glucose.

Total starch and resistant starch contents were determined by incubating 0.1 mL of hydrolysed samples with 3.0 mL GOPOD reagent [glucose oxidase plus peroxidase and 4-aminoantipyrine in reagent buffer (4-hydroxybenzoic acid), at 50 °C for 20 min, where the D-glucose was oxidised to D-gluconate, which was quantitively measured in a colorimetric reaction. The absorbance for each sample and D-glucose controls was read at 510 nm against the reagent blank using UV tolerant cuvettes (Sarstedt Limited, Leicester, UK) and a Lambda UV/Vis spectrophotometer (Perkin-Elmer, Buckinghamshire, UK).

Starch structural analysis- SEC and ^{13}C CP/MAS NMR

SEC analysis was conducted on debranched, purified starch samples using a Waters Advanced Polymer Characterisation System as described in.

Solid-state ^{13}C CP/MAS NMR experiments on all pea and flour powder samples were carried out on a Bruker Avance III 300 MHz spectrometer, equipped with an HXY 4-mm probe, spun at a frequency of 12 kHz, at a ^{13}C frequency of 75.47 MHz, and MAS of 54.7°. Samples were manually ground using a mortar and pestle and approximately 110–130 mg of each sample was packed into a 4-mm cylindrical partially-stabilised zirconium oxide (PSZ) rotor with a Kel-F end cap. The ^{13}C CP-MAS NMR experimental acquisition and processing parameters were 90° 1H rf pulse width of 3.50 µs and 90° 13C rf pulse width of 4.50 µs, contact time of 1000

889 µs, recycle delay of 5 s, spectral width of 22.7 kHz (301.1 ppm), acquisition time of 28.16 ms,
890 time domain points (i.e. size of FID) of 1280, line broadening was set to 20, 6144 number of
891 scans and 16 dummy scans. All experiments were referenced to tetramethylsilane (Brouns et
892 al.) and hexamethylbenzene for ^{1}H and ^{13}C, respectively, and carried out at approximately 26
893 °C.

894 Calculation of starch molecular (double helical) order was performed following the procedure
895 described by Flanagan and colleagues (2015). In brief, following obtaining of free induction
896 decay of all samples, the obtained data was Fourier transformed, phase corrected and zero-
897 filled to 4096 data points. Chemical shift vs relative intensity data was used to obtain an
898 estimation of the total crystallinity of each sample analysed using partial least squares analysis
899 against a reference set of 114 spectra of starch with known values of molecular order obtained
900 using spectral deconvolution and referenced against x-ray diffraction data.

901 Particle size

902 Pea chunk size (cooked) was determined after gastric and intestinal simulated digestion by
903 dynamic light scattering (DLS), using an LS13320 laser diffraction particle size analyser
904 (Beckman-Coulter, Buckinghamshire, UK), using starch as the optical model with PIDS
905 (Polarization Intensity Differential Scattering) obscuration ≥45%. The mean particle size
906 distribution was measured 3 times over 60 second intervals.

907 Microscopy

908 Microscopy was used to characterise the peas and flour throughout the digestion process; to
909 visualise any changes to the macro and microstructure of the foods. It was particularly
910 important to image areas of damaged tissue from the action of chewing, as these areas were
911 accessible to enzymes and therefore would be susceptible to digestion.

912 Light microscopy

913 Light microscopy was used to characterise the macro and microstructure of pea seeds and flour.
914 Uncooked flour samples were hydrated in ultrapure water 20 min before imaging; cooked and
915 digested flour samples were imaged immediately after cooking and digestion steps. Iodine
916 (0.2% iodine in 2% potassium iodide, aqueous) was used to stain starch.
917 Uncooked, cooked and digested pea chunks of approximately $1mm^3$ were fixed in 2.5%
918 glutaraldehyde/2% formaldehyde in 0.1M PIPES buffer for 8 days, to improve starch

polymerisation, because using just 2.5% glutaraldehyde alone was not adequate for *RR* starch. The pea chunks were washed 3 times in 0.1M PIPES buffer for 15 minutes each. The chunks were then post-fixed in 1% osmium tetroxide (aqueous) for 2.5 hours before 3x15-minute ultrapure water washes and an ethanol series dehydration (10, 20, 30, 40, 50 ,60, 70, 80, 90, 100%) with at least 15 minutes between ethanol changes. The final ethanol change was repeated twice more with 100% ethanol. The last ethanol wash was replaced with a 1:1 mix of LR White medium grade resin (London Resin Company Ltd) to 100% ethanol and put on a rotator for an hour. This was followed by a 2:1 and a 3:1 mix of LR White resin to 100% ethanol and finally 100% resin, with at least an hour on the rotator between each change. After 1 hour in 100%, the resin was changed twice more with fresh 100% resin with periods of at least 8 hours on the rotator between changes. Four blocks from each sample were each put into BEEM capsules with fresh resin and polymerised overnight at 60°C. Semi-thin sections approximately 1µm thick were cut using an ultramicrotome (Ultracut E, Reichert-Jung) with a glass knife mounted with an ultrapure water-filled trough. The sections were picked up and transferred onto a drop of water on a glass slide and dried in an oven at 100°C. The sections were then stained with toluidine blue (1% toluidine blue in 1% sodium borate, aqueous) for protein and iodine (0.2% iodine in 2% potassium iodide, aqueous) for starch for only a few seconds and then rinsed with water before being dried again in the oven. The slides were then ready to view under the microscope (Olympus BX60 microscope).

Scanning electron microscopy (SEM)

Pea chunks were fixed using a 2.5% glutaraldehyde/0.1M PIPES buffer (pH 7.4) for 5 days. After washing with 0.1M PIPES buffer, the chunks were dehydrated in a series of ethanol solutions (10, 20, 30, 40, 50, 60, 70, 80, 90, 3x 100%) and 3x 100% ethanol. Samples were critical point dried in a Leica EM CPD300 critical point drier using liquid carbon dioxide as the transition fluid and mounted onto SEM stubs with silver paint (Agar Scientific, Stansted, UK). The samples were coated with gold in an Agar high resolution sputter-coater apparatus. Scanning electron microscopy was carried out using a Zeiss Supra 55 VP FEG SEM, operating at 3kV.

Statistical Analysis

Data were analysed using Graph Pad Prism (GraphPad Software, San Diego, CA, USA), IBM SPSS (Statistics for Windows, Version 24, Armonk, NY, USA) or Mat lab version R2014a,

The Mathworks, Inc.; Natwick, MA). Data were tested for normality using Shapiro-Wilk Test. Comparison of time series data was carried out by two-way analysis of variance (ANOVA) with post hoc LSD Fisher correction. Comparison between groups was carried out by paired Student's *t*-test. All results and graphs are expressed as mean ±SEM. Results were considered statistically significant when $p<0.05$, two sided with the significance level indicated as *$p<0.05$, **$p<0.01$, ***$p<0.001$. All data that support the findings of the study have been deposited in Mendeley Database: (https://data.mendeley.com/datasets/g8cpyyyp3n/draft?a=3bd91ae0-42ba-4d55-8751-d9ba0adeaade).

Supplemental Materials

Supplemental Tables

Table S1. Demographic characteristics of volunteers recruited and completed Study 1[1]

Characteristics All (n=10)	Screening	Visit 1	Visit 2	Visit 3	Visit 4	*P Value*
Gender (M: F)	3:7					
Age (years)	49.3 ±8.5					
Weight (kg)	68.0 ±4.1	67.3±4.1	67.5±4.2	68.0±4.1	68.0±3.9	0.26
BMI (kg/m^2)	24.0 ±0.2	23.8 ±0.1	23.9 ±0.1	24.3 ±0.1	24.2 ±0.2	0.38
Body Fat (%)	27.4 ±7.1	27.4 ±1.7	27.7 ±2.0	27.5 ±1.6	27.6 ±1.6	0.44

[1] Results presented as mean ±SEM

Table S2. Demographic characteristics of volunteers recruited and completed Study 2[1]

Characteristics All (n=12)	Mean of 4 Consecutive Visits
Gender (M: F)	7:5
Age (years)	45.8 ± 4.4
Weight (kg)	69.5 ± 1.9
BMI (kg/m^2)	24.4 ± 0.6
Body Fat (%)	22.9 ± 2.4

[1] Results presented as mean ±SEM

Table S3. Amylopectin/Maltotriose/Maltose found in gastric samples associated with differences found in the RM-MCCV-PLS-DA model between the consumption of *RR* and *rr* peas[1]

***RR* and *rr* Peas Gastric Samples at 30 minutes**				
Metabolite	**Chemical Shift (multiplicity)**	**Association t=30**	**P-Value for Peas t=30**	**Q-Value for Peas t=30**
Amylopectin/Maltotriose /Maltose	5.42(d), 3.60(Chiasson et al.), 3.57(Chiasson et al.), 3.44(Chiasson et al.), 3.29 (Chiasson et al.)	↑[1]	0.000453	0.0024

[1]Sign of association; ↑ Indicates higher excretion with RR, Multiplicity key is as follows: d – doublet, dd – doublet of doublets

977

978 **Table S4. ^{1}H and ^{13}C NMR peak assignments for amylopectin, maltotriose, maltose**

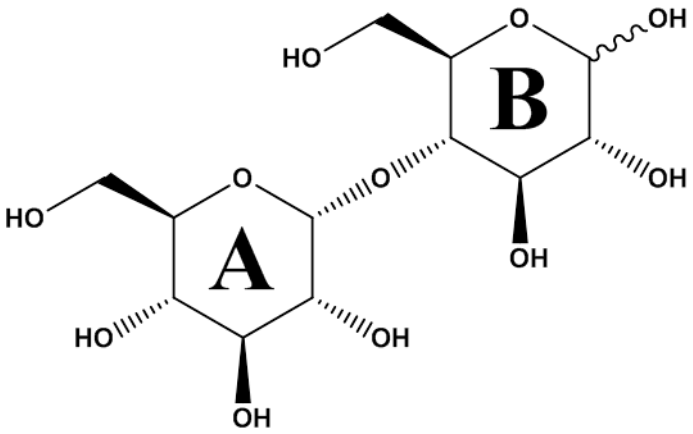

979

980 Maltose backbone

Name	^{1}H NMR: δ_H (ppm)	^{13}C NMR: δ_C (ppm)	Multiplicity and type of protons[a]
Amylopectin			
Maltose units with lineal 1→4	5.35-5.39	102.58	4d, CHs
linkage	4.98	100.98	d, CH
Branching unit with 1→6 linkage	3.62[c]	~	~
(C_1,H_1)	~	75.98[d]	~
Glucan moieties from branching at	5.00-5.01	100.75	2d, CHs
position 6 (C_1,H_1)	3.85[c]	~	~
	~	72.16[d]	~
□/□-Maltotriose and α/β-Maltose[b]			
Ring A			
	3.42-3.46	72.16	3dd, CHs
	3.59	74.36	dd, CH
	3.60	74.46	dd, CH
	3.69	75.74	dd, CH
	3.71	75.54	dd, CH
	3.79	63.19	dd, CH_2
	3.86	63.27	dd, CH_2
	3.92	63.51	dd, CH_2
	3.96	75.98	dd, CH[e]
	3.98	75.99	dd, CH
	5.42	102.28	d, CH
Ring B			
	3.26	76.93	dd, CH[e]
	3.29	76.94	dd, CH
	3.78	78.89	dd, CH
	3.78	63.43	dd, CH_2
	3.79	63.28	dd, CH_2
	4.66	~	d[e]
	4.67	98.50	d, CH

[a]Multiplicity key is as follows: d – doublet, dd – doublet of doublets; CH_2 – methylene, CH - methine protons. [b]□/□-Maltotriose and □/□-maltose can be free and/or as subunits within the chemical structure of amylopectin. [c]Homonuclear correlations observed via DQF- and TQF-COSY experiments. [d]Heteronuclear correlations observed via HMBC experiment. [e]Signals with low intensity. Human Metabolome Data Base (HMDB; http://hmdb.ca/) and literature (Falk and Stanek, 1997) were used for confirmation of assignments.

Table S5. Glucose found in small intestinal samples associated with differences found in the RM-MCCV-PLS-DA model between the consumption of *RR* and *rr* peas[1]

***RR* and *rr* Peas Small Intestinal Samples at 60 minutes**				
Metabolite	**Chemical Shift (multiplicity)**	**Association t=60**	**P-Value for Peas t=60**	**Q-Value for Peas t=60**
Glucose	3.25 (dd), 3.42 (m), 3.49 (m), 3.54 (dd), 3.74 (m), 3.84 (m), 3.91 (dd), 4.65 (d), 5.24 (d)	↑[1]	0.002	0.017

[1]Sign of association; ↑ Indicates higher excretion with RR, Multiplicity key is as follows: d – doublet, dd – doublet of doublets, m – (other) multiplet

Table S6. List of metabolites found in gastric samples associated with differences found in the RM-MCCV-PLS-DA model between the consumption of *RR* and *rr* flour at 15' and 30' post ingestion[1]

***RR* and *rr* Flour Gastric Samples at 15 minutes**				
Metabolite	**Chemical Shift (multiplicity)**	**Association t=15**	**P-Value for Flour t=15**	**Q-Value for Flour t=15**
Amylopectin/Maltotriose /Maltose	5.42(d), 3.60 (dd), 3.57 (dd), 3.44(dd), 3.29 (dd)	↑[1]	0.00005	0.00198
Alanine	1.48 (d)	↓[1]	0.00148	0.02060
Sucrose	3.49 (t),3.58 (dd), 3.79 (t), 3.84(br), 3.91 (m), 4.06(t), 4.23 (d), 5.42 (d)	↓[1]	0.00012	0.00303

[1]Sign of association; ↑ Indicates higher excretion with RR, ↓ Indicates higher excretion with rr. Multiplicity key is as follows: d – doublet, dd – doublet of doublets, m – (other) multiple, br - (broader)

Table S7. List of metabolites found in small intestinal samples associated with differences found in the RM-MCCV-PLS-DA model between the consumption of *RR* and *rr* flour[1]

***RR* and *rr* Flour Small Intestinal Samples at 60 minutes**				
Metabolite	**Chemical Shift (multiplicity)**	**Association t=60**	**P-Value for Flour t=60**	**Q-Value for Flour t=60**
Glucose	3.25 (dd), 3.42 (m), 3.49 (m), 3.54 (dd), 3.74 (m), 3.84 (m), 3.91 (dd), 4.65 (d), 5.24 (d)	↑[1]	0.00009	0.00041
Sucrose	3.49 (t), 3.58 (dd), 3.79 (t), 3.84 (br), 3.91 (m), 4.06 (t), 4.23 (d), 5.42 (d)	↓[1]	0.00033	0.00123
Gamma Amino N-butyrate	2.30(t), 3.02(t)	↓[1]	0.00007	0.00035
Alanine	1.48 (d)	↓[1]	0.00611	0.01429

[1]Sign of association; ↑ Indicates higher excretion with RR, ↓ Indicates higher excretion with rr. Multiplicity key is as follows: d – doublet, dd – doublet of doublets, m – (other) multiple, br - (broader)

Suppl. Table 8. Demographic Characteristics of volunteers recruited and completed Study 3[1]

Characteristics All (n=10)	Visit 1	Visit 2	Visit 3	Visit 4	*P Value*
Gender (M: F)	4:6				
Age (years)	45.4 ±4.85				
Weight (kg)	70.9 ±2.5	70.1 ±2.5	69.4 ±3.3	69.2 ±2.8	0.25
BMI (kg/m^2)	24.0 ±0.9	24.0 ±0.9	24.2 ±1.0	24.0 ±0.9	0.26
Body Fat (%)	28.4 ±1.8	27.7 ±2.0	27.2 ±1.8	27.6 ±6.7	0.28

[1] Results presented as mean ±SEM

Table S9. Demographic Characteristics of volunteers recruited and completed Study 4[1]

Volunteers (n=25)	Screening	Supplementation Period *RR*		Supplementation Period *rr*		Group x Time P Value
		Baseline (Week 0) Visit 1	Baseline (Week 4) Visit 2	Baseline (Week 0) Visit 1	Baseline (Week 4) Visit 2	
Gender (M: F)	10:15	-	-	-	-	-
Age (years)	56.9 ±1.3	-	-	-	-	-
Weight (kg)	71.6 ±2.2	71.7 ±2.2	72.4 ±2.2	71.9 ±2.2	72.0 ±2.2	0.08
BMI (kg/m^2)	24.8 ± 0.5	24.8 ±0.5	25.0 ±0.5	24.9 ±0.5	25.0 ±0.5	0.78
Body Fat (%)	27.1 ±1.5	27.2 ±1.4	27.2 ±1.5	27.1 ±1.5	27.0 ±1.5	0.91

[1] Results presented as mean ±SEM

1011 **Table S10**. Changes in plasma glucose, serum insulin, GLP-1, lipids and HOMA 2 biomarkers following 28 days of *RR* (control) or *rr* pea products
1012 supplementation. ^24 volunteers and ^^22 volunteers included in the calculations.

1013

1014

	RR Line (n=25)			*rr Line (n=25)*			*Mixed Anova*	
	Pre	***Post***	***P Value***	***Pre***	***Post***	***P Value***	***Time P Value***	***Group x Time P Value***
Laboratory Outcomes								
Mean Fasting Glucose (mmol/L)	5.17 ± 0.10	5.22 ± 0.10	0.45	5.11 ± 0.09	5.20 ± 0.09	0.21	0.23	0.86
PPG^ (0-300 min) (mmol/L) ^	5.68 ± 0.13	5.63 ± 0.10	0.70	5.61 ± 0.28	5.80 ± 0.19	0.25	0.21	0.21
Mean Fasting Insulin (µU/mL)	9.37 ± 0.82	9.10 ± 0.96	0.37	8.82 ± 0.82	9.21 ± 0.76	0.30	0.81	0.17
Postprandial Insulin^ (0-300 min) (µU/mL) ^	37.12 ± 3.37	34.25 ± 3.45	0.12	35.37 ±3.09	34.78 ±2.14	0.79	0.23	0.45
Mean Fasting C Peptide (pmol/L) ^^	493 ± 38.35	497 ± 46.79	0.82	463 ± 35.14	498 ± 38.43	0.14	0.25	0.30
GLP-1 (pmol/L) ^	57.44 ± 1.57	59.95 ± 2.19	0.20	59.03 ± 1.99	58.74 ± 2.22	0.83	0.40	0.19
Cholesterol (mmol/L) ^	5.25 ± 0.9	4.91 ± 0.7	0.01	5.16 ± 0.8	5.00 ± 0.7	0.23	0.03	0.22
Triglycerides (mmol/L) ^	0.90 ± 0.07	0.86 ± 0.07	0.23	0.86 ± 0.07	0.88 ± 0.08	0.70	0.66	0.37
LDL Cholesterol (mmol/L) ^	3.28 ± 0.16	2.94 ± 0.14	0.004	3.16 ± 0.15	3.04 ± 0.13	0.22	0.01	0.05
HDL Cholesterol (mmol/L) ^	1.54 ± 0.07	1.58 ± 0.07	0.31	1.60 ± 0.08	1.56 ± 0.07	0.27	0.92	0.11
HOMA2 Beta Cell Function (%B)	91.73 ± 4.56	88.94 ± 4.63	0.19	90.85 ± 5.64	90.96 ± 5.02	0.96	0.36	0.33
HOMA2 Insulin Resistance	1.06 ± 0.08	1.04± 0.10	0.21	1.00 ±0.09	1.05 ± 0.09	0.12	0.45	0.05
HOMA2 Insulin Sensitivity (%S	109 ± 9.02	113 ± 9.35	0.25	120.6 ± 12.1	110.68 ± 8.76	0.32	0.96	0.11

Data are presented as mean ±SEM.

Supplemental Figures

Figure S1. Effect between genotypes (*RR* peas-flour, *rr* peas-flour) after acute consumption of 50 g dry weight of products on plasma glucose and insulin responses. (A, B) Plasma glucose and corresponding serum insulin between *RR* whole pea seeds and flour. (C, D) Plasma glucose and corresponding serum insulin between *rr* whole pea seeds and flour. Repeated Measures Anova model was used for testing time course data with pea seeds and flour and time as factors. LSD Fisher post-hoc tests were performed between timepoints. Paired *t*-tests were used for iAUCs calculations. Normality was checked using Shapiro-Wilk test. Insets show the iAUC between 0 and 180/120 min. Timepoints at which values differed significantly, *p<0.05, **p<0.01, ***p<0.001. The data presented as mean ±SEM (n=11).

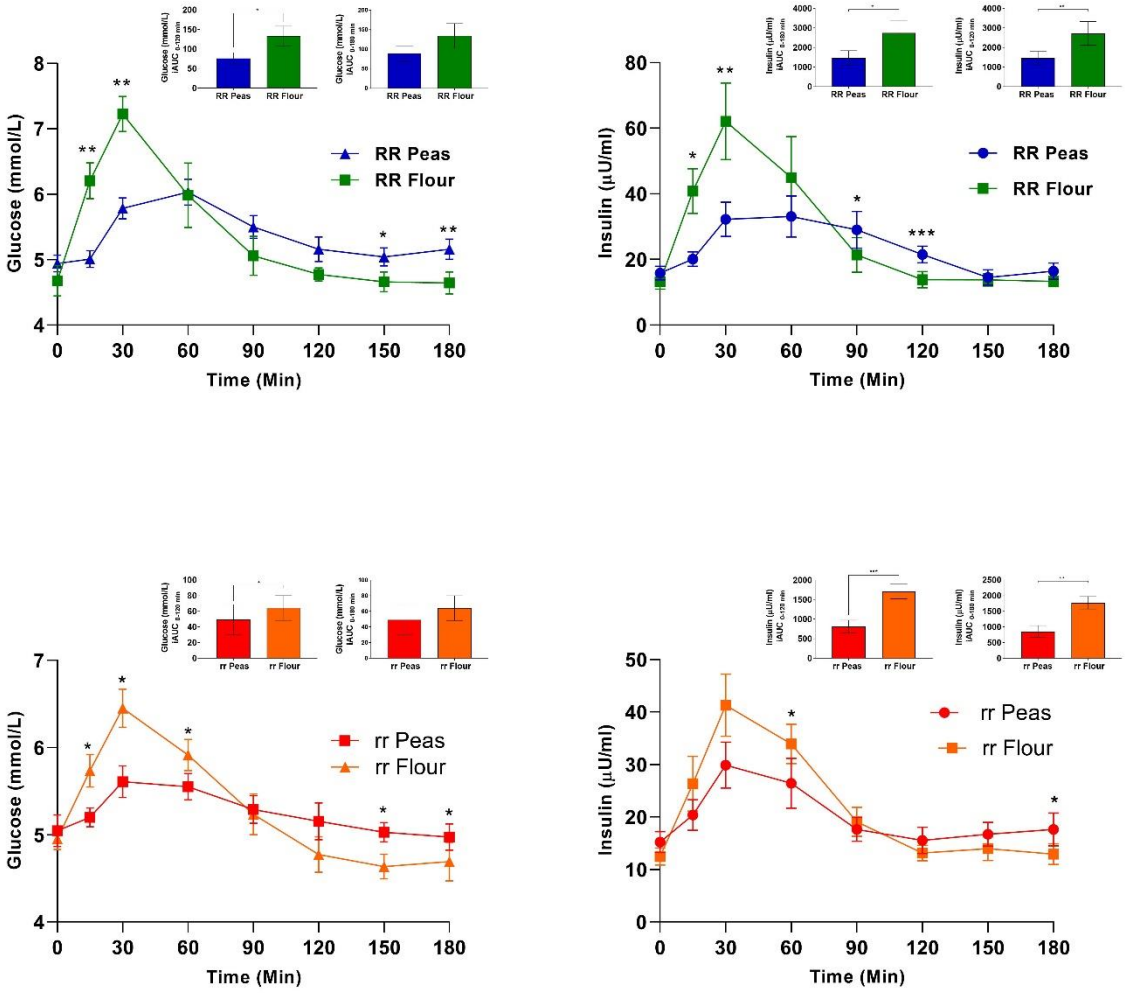

Figure S2. ^{1}H- ^{13}C CP/MAS NMR spectral overlay of uncooked and cooked peas of the *RR* genotype (A) and uncooked and cooked peas of the *rr* genotype (B), with ^{13}C nuclear assignment and inlay of starch glucose monomer

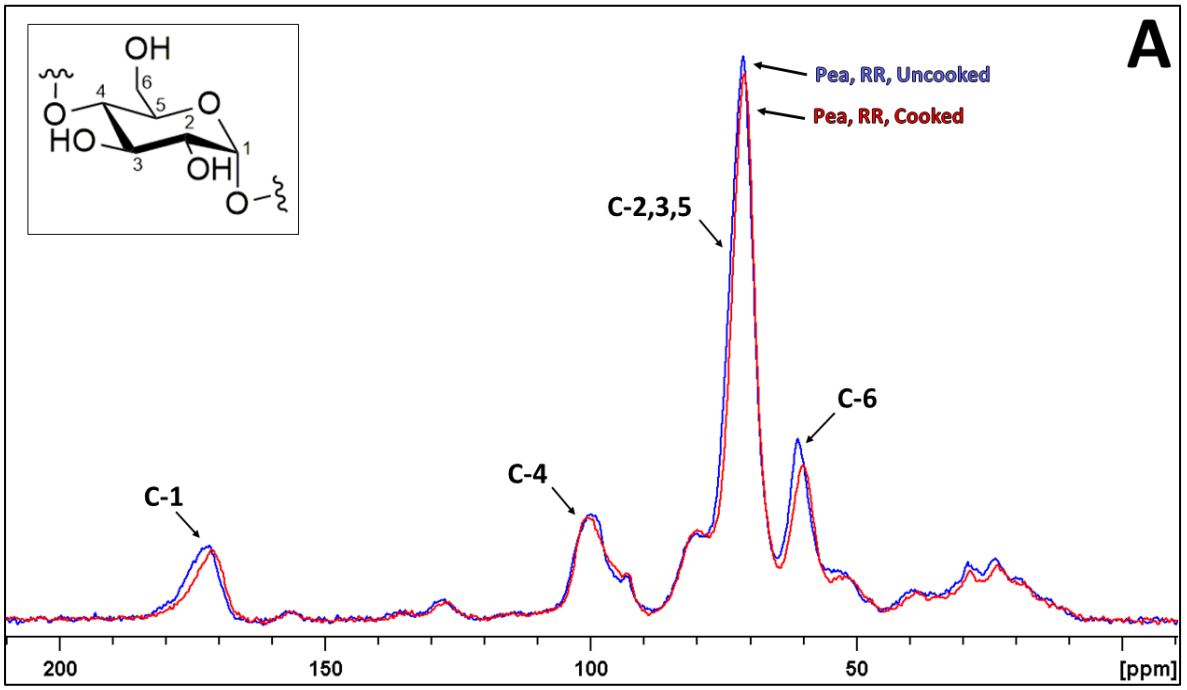

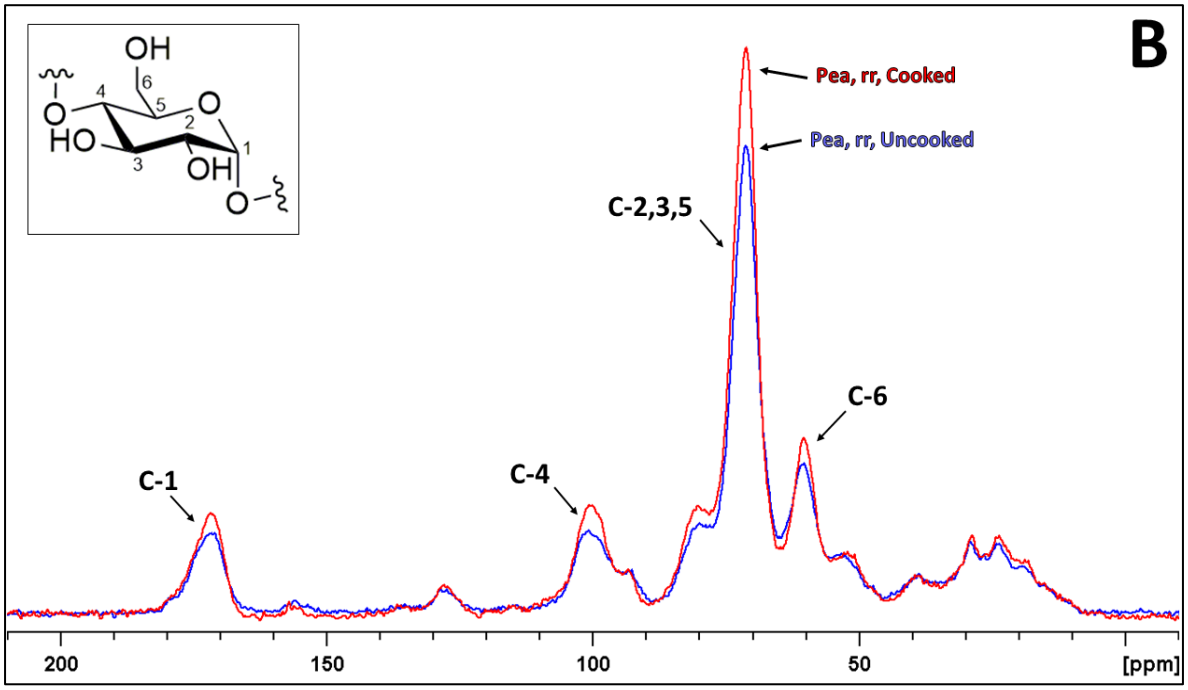

Figure S3. Light micrographs of cooked flour and peas post-simulated digestion;(A) *RR* flour, (B) *rr* flour, (C) *RR* peas, (D) *rr* peas (tissue section). All samples were stained using iodine.

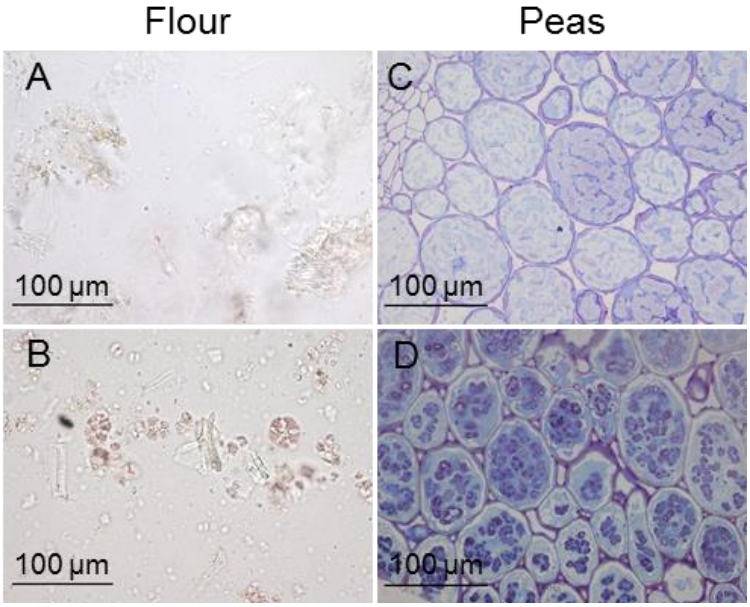

Figure S4. Scanning electron micrographs of uncooked and cooked wholes peas, demonstrate the extent of starch gelatinization within cotyledon cells.

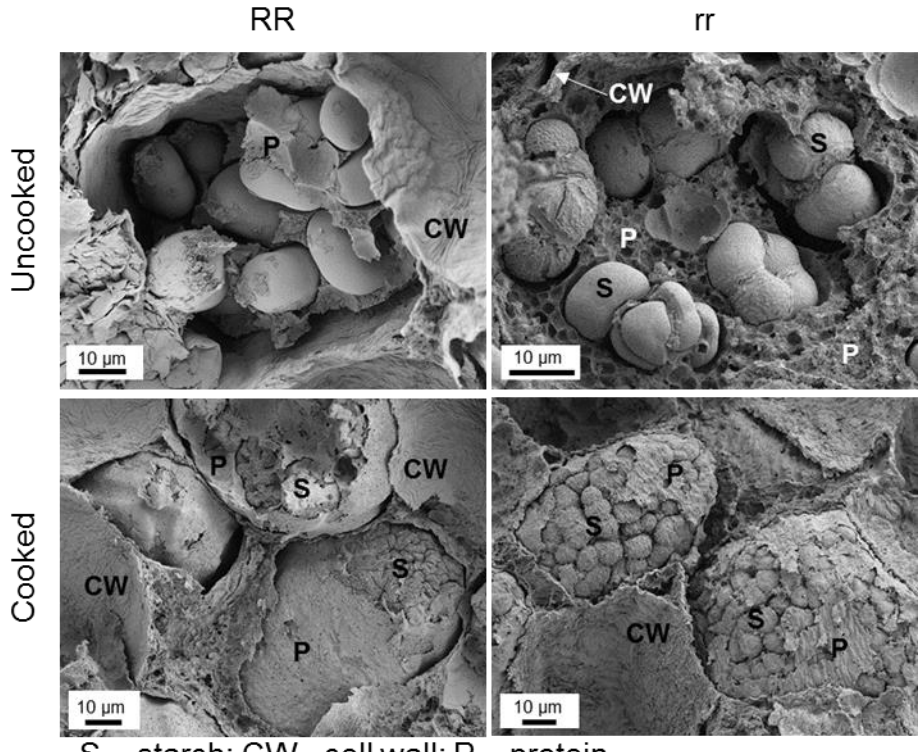

Figure S5. Distribution of the values obtained from the Intensity per nm2 and time (diffusion rate constant) of AA in *RR* and *rr* cooked pea seeds

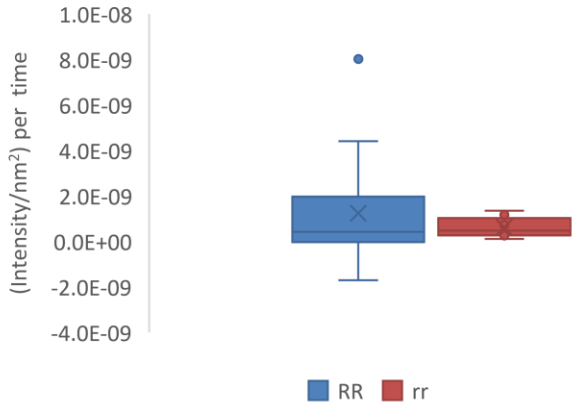

Figure S6. Consort diagram of the long-term study

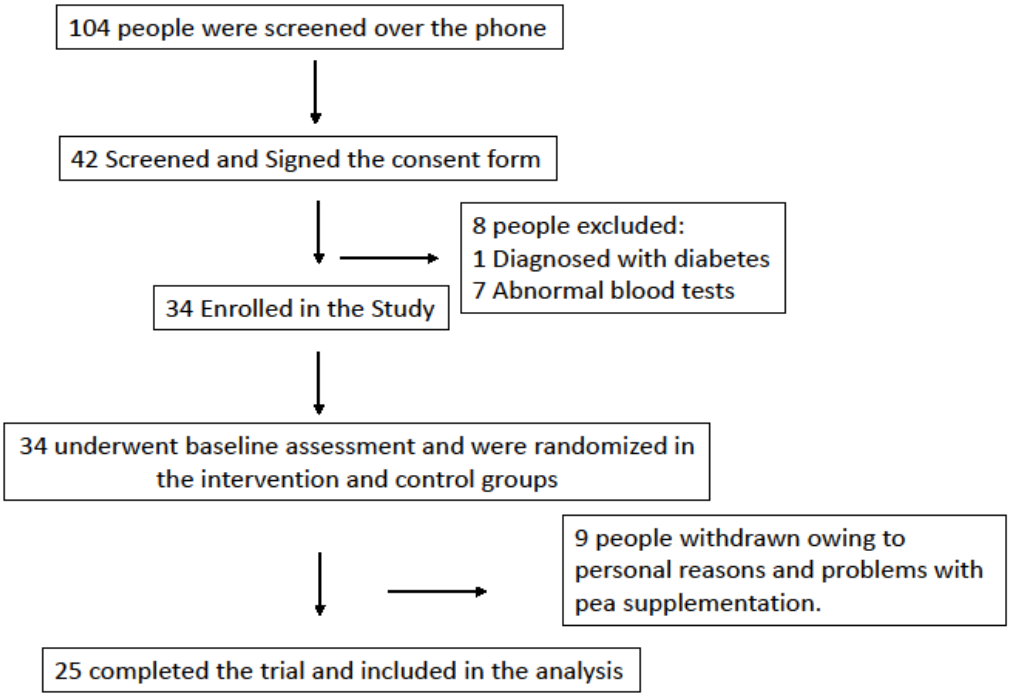

Figure S7. Trigonelline values measured at baseline and follow up visit indicating participants adherence to the (I) *RR* peas and (J) *rr* peas supplementation.

nt

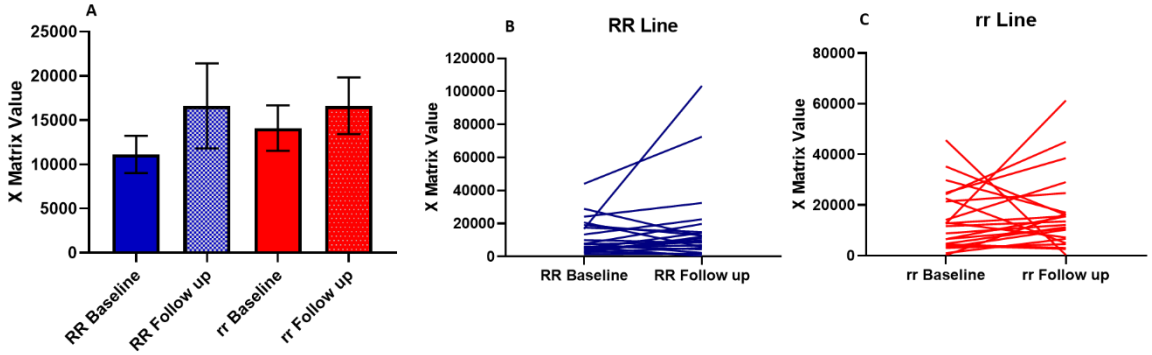

References

BHATTACHARYYA, M. K., SMITH, A. M., ELLIS, T. N., HEDLEY, C. & MARTIN, C. 1990. The wrinkled-seed character of pea described by Mendel is caused by a transposon-like insertion in a gene encoding starch-branching enzyme. *Cell,* 60**,** 115-122.

BOGRACHEVA, T. Y., DAVYDOVA, N., GENIN, Y. V. & HEDLEY, C. 1995. Mutant genes at the r and rb loci affect the structure and physico-chemical properties of pea seed starches. *Journal of experimental botany,* 46**,** 1905-1913.

BROUNS, F., BJORCK, I., FRAYN, K., GIBBS, A., LANG, V., SLAMA, G. & WOLEVER, T. 2005. Glycaemic index methodology. *Nutrition research reviews,* 18**,** 145-171.

CAPORASO, J. G., LAUBER, C. L., WALTERS, W. A., BERG-LYONS, D., LOZUPONE, C. A., TURNBAUGH, P. J., FIERER, N. & KNIGHT, R. 2011. Global patterns of 16S rRNA diversity at a depth of millions of sequences per sample. *Proceedings of the national academy of sciences,* 108**,** 4516-4522.

CHIASSON, J.-L., JOSSE, R. G., GOMIS, R., HANEFELD, M., KARASIK, A., LAAKSO, M. & GROUP, S.-N. T. R. 2003. Acarbose treatment and the risk of cardiovascular disease and hypertension in patients with impaired glucose tolerance: the STOP-NIDDM trial. *Jama,* 290**,** 486-494.

DESSAU, R. & PIPPER, C. B. 2008. "R"--project for statistical computing. *Ugeskrift for laeger,* 170**,** 328-330.

DONOHOE, D. R., GARGE, N., ZHANG, X., SUN, W., O'CONNELL, T. M., BUNGER, M. K. & BULTMAN, S. J. 2011. The microbiome and butyrate regulate energy metabolism and autophagy in the mammalian colon. *Cell metabolism,* 13**,** 517-526.

EDWARDS, C., ZAVOSHY, R., KHANNA, S., SLATER, C., MORRISON, D., PRESTON, T. & WEAVER, L. 2002. Production of 13C labelled pea flour for use in human digestion and fermentation studies. *Isotopes in environmental health studies,* 38**,** 139-147.

EDWARDS, C. H., GRUNDY, M. M., GRASSBY, T., VASILOPOULOU, D., FROST, G. S., BUTTERWORTH, P. J., BERRY, S. E., SANDERSON, J. & ELLIS, P. R. 2015. Manipulation of starch bioaccessibility in wheat endosperm to regulate starch digestion, postprandial glycemia, insulinemia, and gut hormone responses: a

randomized controlled trial in healthy ileostomy participants, 2. *The American journal of clinical nutrition,* 102**,** pp.791-800.

EDWARDS, C. H., MAILLOT, M., PARKER, R. & WARREN, F. 2018. A comparison of the kinetics of in vitro starch digestion in smooth and wrinkled peas by porcine pancreatic alpha-amylase. *Food chemistry,* 244**,** pp.386-393.

FALK, H. & STANEK, M. 1997. Two-dimensional 1 H and 13 C NMR spectroscopy and the structural aspects of amylose and amylopectin. *Monatshefte für chemie/chemical monthly,* 128**,** 777-784.

GARCIA-PEREZ, I., POSMA, J. M., CHAMBERS, E. S., NICHOLSON, J. K., C. MATHERS, J., BECKMANN, M., DRAPER, J., HOLMES, E. & FROST, G. 2016. An analytical pipeline for quantitative characterization of dietary intake: application to assess grape intake. *Journal of agricultural food chemistry,* 64**,** 2423-2431.

GHOOS, Y. F., MAES, B. D., GEYPENS, B. J., MYS, G., HIELE, M. I., RUTGEERTS, P. J. & VANTRAPPEN, G. 1993. Measurement of gastric emptying rate of solids by means of a carbon-labeled octanoic acid breath test. *Gastroenterology,* 104**,** 1640-1647.

GIDLEY, M., COOKE, D., DARKE, A., HOFFMANN, R., RUSSELL, A. & GREENWELL, P. 1995. Molecular order and structure in enzyme-resistant retrograded starch. *Carbohydrate polymers,* 28**,** 23-31.

GREENWOOD, D. C., THREAPLETON, D. E., EVANS, C. E., CLEGHORN, C. L., NYKJAER, C., WOODHEAD, C. & BURLEY, V. J. 2013. Glycemic index, glycemic load, carbohydrates, and Type 2 diabetes: systematic review and dose–response meta-analysis of prospective studies. *Diabetes care,* 36**,** 4166-4171.

HAZARD, B., ZHANG, X., COLASUONNO, P., UAUY, C., BECKLES, D. M. & DUBCOVSKY, J. 2012. Induced mutations in the starch branching enzyme II (SBEII) genes increase amylose and resistant starch content in durum wheat. *Crop science,* 52**,** 1754-1766.

JENKINS, D., WOLEVER, T., TAYLOR, R. H., BARKER, H., FIELDEN, H., BALDWIN, J. M., BOWLING, A. C., NEWMAN, H. C., JENKINS, A. L. & GOFF, D. V. 1981. Glycemic index of foods: a physiological basis for carbohydrate exchange. *The American journal of clinical nutrition,* 34**,** 362-366.

JENKINS, D. J., KENDALL, C. W., AUGUSTIN, L. S., FRANCESCHI, S., HAMIDI, M., MARCHIE, A., JENKINS, A. L. & AXELSEN, M. 2002. Glycemic index: overview

of implications in health and disease. *The American journal of clinical nutrition,* 76**,** 266S-273S.

JENKINS, D. J., KENDALL, C. W., MCKEOWN-EYSSEN, G., JOSSE, R. G., SILVERBERG, J., BOOTH, G. L., VIDGEN, E., JOSSE, A. R., NGUYEN, T. H. & CORRIGAN, S. 2008. Effect of a low–glycemic index or a high–cereal fiber diet on type 2 diabetes: A randomized trial. *Jama,* 300**,** 2742-2753.

KELLINGRAY, L., TAPP, H. S., SAHA, S., DOLEMAN, J. F., NARBAD, A. & MITHEN, R. F. 2017. Consumption of a diet rich in Brassica vegetables is associated with a reduced abundance of sulphate-reducing bacteria: A randomised crossover study. *Molecular nutrition food research,* 61**,** 1600992.

LAMBETH, S. M., CARSON, T., LOWE, J., RAMARAJ, T., LEFF, J. W., LUO, L., BELL, C. J., SHAH, V. O. & OBESITY 2015. Composition, diversity and abundance of gut microbiome in prediabetes and type 2 diabetes. *Journal of diabetes,* 2**,** 1.

LINDSTRÖM, J., PELTONEN, M., ERIKSSON, J., ILANNE-PARIKKA, P., AUNOLA, S., KEINÄNEN-KIUKAANNIEMI, S., UUSITUPA, M., TUOMILEHTO, J. & STUDY, F. D. P. 2013. Improved lifestyle and decreased diabetes risk over 13 years: long-term follow-up of the randomised Finnish Diabetes Prevention Study (DPS). *Diabetologia,* 56**,** 284-293.

LOPEZ-RUBIO, A., FLANAGAN, B. M., SHRESTHA, A. K., GIDLEY, M. J. & GILBERT, E. P. 2008. Molecular rearrangement of starch during in vitro digestion: toward a better understanding of enzyme resistant starch formation in processed starches. *Biomacromolecules,* 9**,** 1951-1958.

MINEKUS, M., ALMINGER, M., ALVITO, P., BALLANCE, S., BOHN, T., BOURLIEU, C., CARRIERE, F., BOUTROU, R., CORREDIG, M. & DUPONT, D. 2014. A standardised static in vitro digestion method suitable for food–an international consensus. *Food function,* 5**,** 1113-1124.

MORRISON, D. J., COOPER, K., WALDRON, S., SLATER, C., WEAVER, L. T. & PRESTON, T. 2004. A streamlined approach to the analysis of volatile fatty acids and its application to the measurement of whole-body flux. *Rapid communications in mass spectrometry,* 18**,** 2593-2600.

O'KEEFE, J. H. & BELL, D. S. 2007. Postprandial hyperglycemia/hyperlipidemia (postprandial dysmetabolism) is a cardiovascular risk factor. *The American journal of cardiology,* 100**,** 899-904.

PANWAR, H., RASHMI, H. M., BATISH, V. K. & GROVER, S. 2013. Probiotics as potential biotherapeutics in the management of type 2 diabetes–prospects and perspectives. *Diabetes/metabolism research reviews,* 29**,** 103-112.

PILICHIEWICZ, A. N., CHAIKOMIN, R., BRENNAN, I. M., WISHART, J. M., RAYNER, C. K., JONES, K. L., SMOUT, A. J., HOROWITZ, M. & FEINLE-BISSET, C. 2007. Load-dependent effects of duodenal glucose on glycemia, gastrointestinal hormones, antropyloroduodenal motility, and energy intake in healthy men. *American journal of physiology-endocrinology metabolism,* 293**,** E743-E753.

PRESTON, T. & MCMILLAN, D. 1988. Rapid sample throughput for biomedical stable isotope tracer studies. *Biomedical environmental mass spectrometry,* 16**,** 229-235.

RAYNER, T., MOREAU, C., AMBROSE, M., ISAAC, P., ELLIS, N. & DOMONEY, C. 2017. Genetic variation controlling wrinkled seed phenotypes in Pisum: how lucky was Mendel? *International journal of molecular sciences,* 18**,** 1205.

SATOH, H., NISHI, A., YAMASHITA, K., TAKEMOTO, Y., TANAKA, Y., HOSAKA, Y., SAKURAI, A., FUJITA, N. & NAKAMURA, Y. 2003. Starch-branching enzyme I-deficient mutation specifically affects the structure and properties of starch in rice endosperm. *Plant physiology,* 133**,** 1111-1121.

SHRESTHA, A. K., NG, C. S., LOPEZ-RUBIO, A., BLAZEK, J., GILBERT, E. P. & GIDLEY, M. 2010. Enzyme resistance and structural organization in extruded high amylose maize starch. *Carbohydrate polymers,* 80**,** 699-710.

SKRABANJA, V., LILJEBERG, H. G., HEDLEY, C. L., KREFT, I. & BJÖRCK, I. M. 1999. Influence of genotype and processing on the in vitro rate of starch hydrolysis and resistant starch formation in peas (Pisum sativum L.). *Journal of agricultural food chemistry,* 47**,** 2033-2039.

TAHIR, R., ELLIS, P. R., BOGRACHEVA, T. Y., MEARES-TAYLOR, C. & BUTTERWORTH, P. 2010. Study of the structure and properties of native and hydrothermally processed wild-type, lam and r variant pea starches that affect amylolysis of these starches. *Biomacromolecules,* 12**,** 123-133.

WANG, Q., GARRITY, G. M., TIEDJE, J. M. & COLE, J. R. 2007. Naive Bayesian classifier for rapid assignment of rRNA sequences into the new bacterial taxonomy. *Applied and enviromental microbiology,* 73**,** 5261-5267.

WANG, S. & COPELAND, L. 2013. Molecular disassembly of starch granules during gelatinization and its effect on starch digestibility: a review. *Food function,* 4**,** 1564-1580.

WANG, T. L., BOGRACHEVA, T. Y. & HEDLEY, C. L. 1998. Starch: as simple as A, B, C? *Journal of experimental botany,* 49**,** pp.481-502.

WOLEVER, T. M. & BOLOGNESI, C. 1996. Source and amount of carbohydrate affect postprandial glucose and insulin in normal subjects. *The journal of nutrition,* 126**,** 2798-2806.

ZHANG, G., AO, Z. & HAMAKER, B. R. 2006. Slow digestion property of native cereal starches. *Biomacromolecules,* 7**,** 3252-3258.

ZHOU, Y., HOOVER, R. & LIU, Q. 2004. Relationship between alpha-amylase degradation and the structure and physicochemical properties of legume starches. *Carbohydrate Polymers*, 57(3) 299-317.

Acknowledgements

We thank Dr Eleutheria Panteliou and Dr Lilian Mendoza for their help during nasogastric and nasoduodenal tubes insertion. We thank Alia Sukkar and Anna Cherta Murillo for their assistance in the randomized controlled trial study and Dr Georgia Franco Becker and Dr Claire Byrne for their help with the radioimmunoassays. We thank Mrs Eleanor McKay for technical assistance with the plasma ^{13}C glucose and urine ^{13}C SCFA assay and Mrs Sandra Small for technical assistance with the breath ^{13}C and urine ^{13}C SCFA assay and growth of isotope labelled pea seeds. We thank Dr Mary Parker for valuable discussions and interpretation of the microscopy images. All clinical trials were conducted at the NIHR/Wellcome Trust Imperial Clinical Research Facility.

The Division of Integrative Systems Medicine and Digestive Disease at Imperial College London receives financial support from the National Institute of Health Research (NIHR) Imperial Biomedical Research Centre (BRC) based at Imperial College Healthcare NHS Trust and Imperial College London, in line with the Gut Health research theme. IGP is supported by a National Institute for Health Research (NIHR) fellowship (NIHR-CDF-2017-10-032). CD gratefully acknowledges support from the Department for Environment, Food & Rural Affairs (CH0103, CH0111, Pulse Crop Genetic Improvement Network; LK09126) and from the Biotechnology and Biological Sciences Research Council (BBSRC; BB/L025531/1, BBS/E/J/000PR9799). The authors also gratefully acknowledge the support of the BBSRC through the BBSRC Institute Strategic Programme Food Innovation and Health BB/R012512/1 and its constituent project(s) BBS/E/F/000PR10343 (Theme 1, Food Innovation) and BBS/E/F/000PR10345 (Theme 2, Digestion in the Upper GI Tract). GF is an NIHR Senior Investigator. This research was funded by the Biotechnology and Biological Sciences Research Council (BBSRC, Grant Nos. BB/L025582/1, BB/L025418/1, BB/L025531/1,

BB/L025566/1). Views expressed in this publication are those of the authors and not necessarily those of the NHS, NIHR, or the Department of Health.

Authors contributions

GSF oversaw the design and implementation of the *in vivo* experiments. ESC designed and applied for ethics of the human studies. KP managed and performed all the experimental studies *in vivo*, samples processing and data analysis. RA and MK assisted in experimental human studies 2 and 3. Metabolomics analysis was performed by KP and IGP. Metabolite identification was performed by IGP and JISC. DJM and TP oversaw the stable isotope analysis and data analysis and labelled crop production (TP). LJS performed simulated digestions, starch analysis of pea seeds and particle size analysis of pea fragments; sample preparation and imaging using light microscopy and sample preparation for scanning electron microscopy. Preparation, sectioning and imaging of pea tissue sections was done by RS and KLC; KLC performed SEM. NP carried out simulated digestions of flours and subsequent starch analysis; diffusion experiments using fluorescence microscopy were also performed by NP. TK and YK carried out solid state NMR experiments. PJW, FW and CE oversaw the design and implementation of the digestions *in vitro* and microscopy studies. CD oversaw field trials of the variant pea lines and multiplication of their seeds, with quality testing for all experiments. KP, JAKM, RCS, and JMB performed 16S rRNA gene sequencing and data analysis. GF and KP led the initial drafts of the manuscript. All authors contributed to the final draft of the manuscript.

Declaration of Interests: None of the authors have a conflict of interest.